Title

Pathological Cardiopulmonary Evaluation of Rats Chronically Exposed to Traffic-Related Air Pollution

Journal

Environmental Health Perspectives, 128(12)

ISSN

0091-6765

Authors

Edwards, Sabrina

Zhao, Gang

Tran, Joanne

et al.

Publication Date

2020-12-01

DOI

10.1289/ehp7045

Peer reviewed

A Section 508–conformant HTML version of this article is available at https://doi.org/10.1289/EHP7045.

Pathological Cardiopulmonary Evaluation of Rats Chronically Exposed to Traffic-Related Air Pollution

Sabrina Edwards,[1] Gang Zhao,[1,2] Joanne Tran,[1,3] Kelley T. Patten,[4] Anthony Valenzuela,[4] Christopher Wallis,[5] Keith J. Bein,[5,6] Anthony S. Wexler,[5,7] Pamela J. Lein,[4] and Xiaoquan Rao[1,8]

[1]Oregon Institute of Occupational Health Sciences, Oregon Health and Science University, Portland, Oregon, USA
[2]Department of Cardiology, Shandong Provincial Hospital affiliated to Shandong University, Jinan, Shandong, P.R. China
[3]University of Portland, Portland, Oregon, USA
[4]Molecular Biosciences, School of Veterinary Medicine, University of California, Davis, Davis, California, USA
[5]Air Quality Research Center, University of California, Davis, Davis, California, USA
[6]Center for Health and the Environment, University of California, Davis, Davis, California, USA
[7]Mechanical and Aerospace Engineering, Civil and Environmental Engineering, and Land, Air and Water Resources, University of California, Davis, Davis, California, USA
[8]Division of Cardiology, Department of Internal Medicine, Tongji Hospital, Tongji Medical College, Huazhong University of Science and Technology, Wuhan, Hubei, P.R. China

Background: Traffic-related air pollution (TRAP) is made up of complex mixtures of particulate matter, gases and volatile compounds. However, the effects of TRAP on the cardiopulmonary system in most animal studies have been tested using acute exposure to singular pollutants. The cardiopulmonary effects and molecular mechanisms in animals that are chronically exposed to unmodified air pollution as a whole have yet to be studied. Additionally, sex-dependent toxicity of TRAP exposure has rarely been evaluated.

Objectives: This study sought to assess the cardiopulmonary effect of chronic exposure to unmodified, real-world TRAP in both female and male rats.

Methods: Four-week-old male and female rats were exposed to TRAP or filtered air for 14 months in a novel facility drawing air from a major freeway tunnel system in Northern California. Inflammation and oxidative stress markers were examined in the lung, heart, spleen, and plasma, and TRAP deposits were quantified in the lungs of both male and female rats.

Results: Elemental analysis showed higher levels of eight elements in the female lungs and one element in the male lungs. Expression of genes related to fibrosis, aging, oxidative stress, and inflammation were higher in the rat hearts exposed to TRAP, with female rats being more susceptible than males. Enhanced collagen accumulation was found only in the TRAP-exposed female hearts. Plasma cytokine secretion was higher in both female and male rats, but inflammatory macrophages were higher only in TRAP-exposed male spleens.

Discussion: Our results in rats suggest pathological consequences from chronic TRAP exposure, including sex differences indicating females may be more susceptible to TRAP-induced cardiac fibrosis. https://doi.org/10.1289/EHP7045

Introduction

Epidemiological studies worldwide have shown that exposure to ambient air pollution is associated with significantly higher incidence of cardiovascular and respiratory diseases contributing to overall global mortality (Brook et al. 2004; Cohen et al. 2017; Ghorani-Azam et al. 2016; Münzel et al. 2017a, 2017b; Newby et al. 2015). Ambient air pollution is a complex mixture of both gaseous [nitric oxides (NO_x), carbon monoxide (CO), lead (Pb), ozone (O_3), sulfur oxides (SO_x), and volatile organic carbons (VOCs)] and solid particulate matter (PM) of various sizes. The particulates are categorized as PM with a diameter of less than 10 μm (PM_{10}), PM with diameter of 2.5 μm or smaller ($PM_{2.5}$), or ultrafine PM less than 0.1 μm in diameter (ultrafine PM or UFPM) (Suh et al. 2000). The composition of air pollution can vary vastly, depending on its source of generation; however, pollutants generated from automobile sources are of high health risk. Traffic-related air pollution (TRAP) is generated from several different sources and has been shown to be exceptionally hazardous to sensitive populations, such as the elderly (Alexeeff et al. 2018) and children (Bates 1995; Calderón-Garcidueñas et al. 2008). Changes in certain elements attributed to TRAP in the mass fraction of $PM_{2.5}$ have been shown to modify risk factors of exposed individuals, making TRAP an important pollutant to examine (Dominici et al. 2015; Schnelle-Kreis et al. 2009). TRAP PM sources include crustal elements (those originating from earth's crust, such as silicon, iron, aluminum, and calcium) and traffic-related elements. Crustal elements generated from the wear of tires on roadways differ from traffic-related elements that originate from multiple motorized sources, including brake pads, diesel combustion, and vehicle machinery (Han and Naeher 2006). In addition, gaseous pollutants interact with PM through complex atmospheric photochemical reactions to form secondary pollutants, such as sulfates and nitrates (Bourdrel et al. 2017).

In 2012, the U.S. Environmental Protection Agency (U.S. EPA) reevaluated the safety threshold for $PM_{2.5}$ and lowered the threshold from 15 $\mu g/m^3$ to 12 $\mu g/m^3$ daily per 1-y interval, but these values have not been reevaluated since then (U.S. EPA 2013). However, although the national average in the United States for overall $PM_{2.5}$ concentration has been decreasing annually (McClure and Jaffe 2018), the World Health Organization has advised that the threshold of $PM_{2.5}$ concentration be no greater than 10 $\mu g/m^3$ because adverse health effects have been observed at concentrations as low as 3–5 $\mu g/m^3$ above ambient background levels (Krzyzanowski and Cohen 2008; World Health Organization Occupational and Environmental Health Team 2006). Exposure to low levels of TRAP may occur daily for individuals living near highways or commuting. As traffic increases in the United States, congestion leads to generation of more TRAP, and as a result, individuals who live near highways or who commute are exposed to moderate levels of TRAP more frequently (Zhang and Batterman 2013). Currently, few studies have evaluated whether chronic exposure to low-dose TRAP

Address correspondence to Xiaoquan Rao, Oregon Institute of Occupational Health Sciences, Oregon Health & Science University, 3181 SW Sam Jackson Park Rd., Portland, OR 97239 USA. Email: raox@ohsu.edu

Supplemental Material is available online (https://doi.org/10.1289/EHP7045).

The authors declare they have no actual or potential competing financial interests.

Received 10 March 2020; Revised 10 November 2020; Accepted 13 November 2020; Published 4 December 2020.

($\leq 12\,\mu g/m^3$ $PM_{2.5}$/d) elicits cardiopulmonary diseases or other adverse health effects. Although epidemiological studies have shown increased risk of cardiopulmonary disease due to air pollution, they are incapable of concluding mechanistically how TRAP induces cardiovascular and respiratory changes. Animal studies are crucial in mechanistically investigating how air pollution induces negative health effects (Bernstein et al. 2004). Contemporary animal research has implicated oxidative stress and inflammation as primary mechanisms inducing cardiovascular and pulmonary diseases following air pollution exposure, particularly exposure to $PM_{2.5}$ produced by diesel and gasoline vehicle emissions (Lodovici and Bigagli 2011).

Because copollutants found in TRAP add confounding variables to mechanistic exploration, many animal studies have focused on isolating specific components of TRAP in highly controlled exposure systems or via intranasal instillation (Shang and Sun 2018). Although this approach allows concise scrutiny of how specific pollutants mediate disease, it does not examine the multifaceted and unique elemental makeup of TRAP to which humans are exposed. The current study focused on using a real-world exposure model via an existing tunnel freeway system, without any modification of any components of TRAP. The air found in the tunnel freeway system contains gases and particles that are emitted by vehicle travel and inhaled by commuters daily (Allen et al. 2001; Gross et al. 2000), and that are representative of daily TRAP exposures for those who live near highways or who commute. Using this unique tunnel exposure facility in Northern California, we tested the hypothesis that chronic exposure to real-world TRAP induces significant cardiopulmonary pathology. After months-long exposure to TRAP (at concentrations not typically examined in many studies), the cardiovascular, immune, and respiratory systems were studied for pathological changes typically observed in air pollution research. Both male and female rats were evaluated to assess the impact of sex on outcome.

Materials and Methods

Animals

This study was a subset of a larger study designed to examine the health impacts of real-time TRAP exposures. All procedures involving animals were conducted in strict compliance to protocols approved by the University of California, Davis (UC Davis) Institutional Animal Care and Use Committee. Wild-type Fischer 344 rats used in this study were derived from mating of Fischer 344 females (obtained from Charles River Laboratories) with hemizygous TgF344-AD male rats (obtained from a colony established at UC Davis since 2016) in the animal facility at UC Davis. Facilities that housed animals, including the tunnel vivarium, were environmentally controlled at 23 ± 3°C, and were on a 12-h light–dark cycle. The animals were housed in regular rat cages with dimensions of 18.75 in × 10.25 in × 8 in (47.63 cm × 26.04 cm × 20.32 cm) and corncob bedding. Standard chow diet (Teklad global 18% protein rodent diet; Envigo) and water were provided *ad libitum*. Postnatal day 28 male and female Fischer 344 rats ($n = 24$) were randomly divided into two sex-matched cohorts, filtered air (FA) and TRAP groups ($n = 6$ per group), using a random number generator.

TRAP Exposure

The tunnel vivarium, adjacent to a heavily trafficked freeway tunnel in Northern California, continuously drafted air from the eastbound exit of the tunnel bores with an air flow rate of 35 cubic feet/min (1 m^3/min) in each chamber (Berg et al. 2020; Patten et al. 2020). Both light-duty and heavy-duty vehicles pass through this tunnel on a regular basis, with a traffic intensity of about 60,000 vehicles/d (Ban-Weiss et al. 2008; Geller et al. 2005). This approach naturally collected vehicular emissions and allowed both light and heavy vehicle traffic pollution to be directly delivered into TRAP exposure chambers in the facility vivarium. Air for the identical but separate FA exposure chambers was drawn from ambient air surrounding the facility and underwent various emission-control protocols to remove residual air pollutants prior to being delivered to animals. In brief, ambient air was sequentially processed using coarse filtration to remove large debris/dust, an activated carbon scrubber [Phresh® HGC701018 Air Carbon Filter; 8 in × 39 in (20.32 cm × 99.06 cm); 950 cubic feet/min (26.9 m^3/min) max flowrate] to remove volatile organic compounds. The flow was then split into three parallel streams, and each stream subjected to an additional inline activated carbon scrubber [Phresh® HGC701180 Inline Air Carbon Filter; 8 in × 24 in (20.32 cm × 60.96 cm); 750 cubic feet/min (21.24 m^3/min) maximum flow rate], followed by three-way catalytic converters (MagnaFlow® 445006; CARB-compliant) to remove nitrogen oxides, hydrocarbons, and carbon monoxide. The flows were then recombined, plumbed to the air flow control systems situated beneath the facility, and then pumped through an inline, custom-made, ultrahigh-efficiency particle filtration system housed inside the instrumentation room for removing ultrafine, fine, and coarse mode PM. The filtration system consisted of six parallel 8-in diameter ducts coupled by inlet and outlet manifolds. Each duct terminated with a stainless-steel wire mesh filter support and Teflon-coated borosilicate glass microfiber filter with woven glass backing (Pallflex® Emfab™ TX40) that were compression sealed to the outlet manifold via quick-disconnect couplings and polytetrafluoroethylene (PTFE) seals. The outlet was then plumbed to an array of sampling ports that directed airflow to: a) the exposure chambers in the vivarium; *b*) the PM samplers in the instrumentation room; and *c*) the air sampling train for air monitoring instrumentation. The average particle number filtration efficiency, average $PM_{2.5}$ mass filtration efficiency, and average total suspended particulate mass filtration efficiency were $97.7\% \pm 0.7\%$, $89\% \pm 5\%$, and $89\% \pm 5\%$ respectively.

The exposure facility, which was located within 50 m of a freeway tunnel, is 44 ft long and 10 ft wide. It was divided into three rooms, one [9 ft × 13 ft (2.7 m × 4.0 m)] for monitoring TRAP and FA pollutant concentrations and the security of the facility, a second [9 ft × 18 ft (2.7 m × 5.5 m)] for the exposure chambers, and a third [9 ft × 12 ft (2.7 m × 3.7 m)] for on-site laboratory work. Each exposure chamber was 12.8 ft × 3 ft × 7.8 ft (3.9 m × 0.9 m × 2.4 m; L × W × H), with 6 shelves, each of which accommodated 18 rat cages with dimensions of 18.75 in × 10.25 in × 8 in (47.63 cm × 26.04 cm × 20.32 cm). One chamber was used for FA exposures and the other for TRAP exposures. All blowers and pumps were housed outside the facility and plumbed through the facility walls, and the exposure chambers were insulated for sound so that the animals did not experience significant stress from roadway and vehicle noise. The TRAP rats were exposed to air drawn directly from the eastbound exit of the tunnel bores continuously without any modification. For the FA exposures, ambient air was drawn from outside near the facility through the filtration process described above. Pollutant concentrations and pressure drops were checked regularly throughout the exposures, and the particle filters for FA exposure were replaced twice throughout the entire exposure duration of this study. At the bottoms of both exposure chambers, the tunnel and FA chambers were plumbed through the wall to separate blowers situated under the facility. A variable frequency drive with PID (proportional-integral-differential) feedback powered the blowers to maintain the flow at the desired value. The blowers maintained a small negative pressure in the exposure chambers that drew air from either the tunnel face for the tunnel chamber, or through the air

cleaning equipment for the FA chamber. Animals were exposed continuously 24 h/d, 7 d/wk for a total of 427 d (~14 months).

Concentrations of $PM_{2.5}$ in $\mu g/m^3$ in the continuous 14-month exposure duration were calculated weekly using a gravimetric method by weighing the PM samplers (PTFE filters - 3 μm, 25 mm, Pall® Teflon) before and after the exposure. At the end of the exposure, animals were transported back to the UC Davis campus, where they were housed for 18 h until euthanized for tissue collection (Figure S1).

TRAP Elemental and Physical Analysis

Chemical and physical characterization of both TRAP and FA exposure chamber atmosphere was conducted via real-time air quality instrumentation and analysis from traditional filter-based sampling and techniques. Particulate matter ($PM_{2.5}$) and Total Suspended Particulate (TSP) concentrations were measured with 5 s resolution via DustTrak DRX Aerosol Monitor (TSI, Model 8533). Continuous 24-h PM filter samples were collected in each of the 8 Interagency Monitoring of Protected Visual Environments (IMPROVE) modules (4 for TRAP and 4 for clean FA labeled A–D, located immediately upstream of the exposure chambers) (Solomon et al. 2014) once every 3 d and were subsequently analyzed to determine mass concentration and composition. The concentration and composition of TRAP, especially pollutants inside the tunnel, largely depend on the traffic condition and topography (Ginzburg et al. 2015; Padró-Martínez et al. 2012) and thus are relatively stable throughout the year. In this study, the filters during the last 3 months of the exposure period were used for the concentration and composition analyses. For both TRAP and FA, modules A–C were configured to collect $PM_{2.5}$ and module D was configured to collect TSP. Sampling flow rates were 23 L/min for modules A–C and 16.9 L/min for module D. PTFE filters (Pall® Teflon 25 mm; 3.0 μm pore size) were used in modules A and D to determine $PM_{2.5}$ mass concentration by gravimetric method and elemental composition by X-ray fluorescence (XRF). Quartz $PM_{2.5}$ filters (Pallflex® tissuquartz; 25 mm) were used in module B to measure elemental and organic carbon (EC/OC) by thermal optical reflectance (TOR) method that applies different temperatures for carbon fractions' measurement through programmed heating in a controlled atmosphere (Chow et al. 2007), and Teflon-coated borosilicate glass microfiber filters (Pallflex® Emfab™ TX40; 37 mm) were used in module C. Gravimetric, XRF, and TOR analyses were performed weekly by the Air Quality Research Center at UC Davis (http://vista.cira.colostate.edu/Improve/particulate-monitoring-network/). In brief, the PTFE filters were weighed before and after sampling in an environmentally controlled weighing chamber (MTL AH500) on a Mettler XP6 microbalance (Mettler-Toledo), and the values were recorded to calculate the mass differences (Air Quality Research Center 2020c). After weighing, PTFE filters that had been sampled in $PM_{2.5}$ modules were prepared for XRF analysis on an Epsilon 5 analyzer (Malvern Panalytical) operated under vacuum. The samples were excited by X-ray generated from a 100 kV side window X-ray tube with a dual Scandium (Sc)/Tungsten (W) anode, and the sample spectrum of X-ray counts vs. energy were analyzed with the Epsilon 5 Software (Air Quality Research Center 2020a). The filter mass differences divided by volume (flow rate × sampling time) were converted to PM concentrations ($\mu g/m^3$), and the elements in terms of counts/mV/s were converted into areal densities, using element calibration factors. The collected data were stored in the UC Davis IMPROVE database (Air Quality Research Center 2020b).

Sample Collection and Extraction

At the conclusion of the exposure period, animals were measured for body weights and then euthanized by exsanguination following deep anesthesia with 4% isoflurane (Southmedic Inc.) administered at a rate of 1.5 L/min. While anesthetized, rats' blood was collected from the heart using K_2EDTA-coated tubes (BD Biosciences) via cardiac puncture. Collected blood samples were put on ice immediately until centrifuged at 1,800 × *g* for 20 min. Plasma was pipetted into individual microcentrifuge tubes and frozen at −80°C. Immediately following cardiac puncture, animals were transcardially perfused with 100 mL of cold 0.1 M phosphate buffered saline (PBS; Gibco) at a rate of 15 mL/min using a Masterflex peristaltic pump (Cole Parmer). The lung, heart, and spleen tissues were removed and weighed using an analytical balance (Mettler Toledo). The heart was transversely cut into three equal pieces once harvested. The middle piece of each heart was embedded in optimal cutting temperature compound (OCT; Sakura Finetek) for frozen sectioning, and the remaining heart tissue was snap frozen and stored at −80°C. Images of fresh entire lung were taken by an iPhone 8 camera at 1 × magnification under the same condition immediately after tissue harvest. The tissues were then snap-frozen by liquid nitrogen and stored at −80°C. The spleen tissue was minced into 2- to 4-mm pieces using a scalpel blade, incubated with red blood cell lysis buffer (BioLegend) for 5 min, centrifuged at 500 × *g* for 5 min at room temperature and resuspended in PBS to obtain the single-cell suspension for flow cytometry.

Tissue Elemental Analysis

Weighed, frozen lung samples were digested with 0.5 (<100 mg) to 1 mL (>100 mg) of concentrated nitric acid (trace metal grade, Fisher) in Sarstedt polypropylene culture tubes (55.516 series, Sarstedt Inc.). Blank samples were prepared with 0.5 mL nitric acid using the same digestion method as the tissue samples. The tubes were loosely capped and digested for 1 h at 90°C using a heating block. After 24 h, samples were diluted 5 times to a final volume of 2,000 μL in 1% nitric acid. The diluted samples were vortexed before analysis via inductively coupled plasma mass spectroscopy (ICP-MS) measurement. All controls were prepared in triplicates with a standardized calibration curve. Measurements and analysis were conducted via ICP-MS performed using an Agilent 7700x equipped with an ASX 500 autosampler. The system was operated at a radio frequency power of 1,550 W, an argon (Ar) plasma gas flow rate of 15 L/min, Ar carrier gas flow rate of 0.9 L/min. Elements were measured with the kinetic energy discrimination mode using Helium gas (4.3 mL/min). Semiquantitative data were collected using a 2-point (0, 100 ppb (ng/g) calibration curve prepared from an element standard (VHG-SM-68-1-100). To further assess accuracy of the semiquantitative calibration curve, a National Institute of Standards and Technology (NIST) reference standard (water, SRM 1643f) was prepared. The detection limit of each element is listed in Table S1. Elemental analysis was performed in the Oregon Health & Science University's (OHSU) Elemental Analysis Core, Portland, Oregon, USA.

Quantitative Real-Time Polymerase Chain Reaction (qRT-PCR)

Frozen lung (right upper lobe) and heart (lower one-third) tissues were homogenized in ceramic beaded tubes (Fisher Scientific) using a Bead Mill 4 homogenizer (Fisher Scientific). Total RNA was extracted from homogenized tissue using TRIzol reagent per protocol provided by manufacturer (Fisher Scientific). Using the High-Capacity cDNA Reverse Transcription Kit (Applied Biosystems) according to manufacturer's protocol, cDNA was synthesized from total RNA via reverse transcription. Quantity and quality of total RNA and cDNA were analyzed by spectrophotometry using Thermo Scientific™ NanoDrop™ One (ThermoFisher). Quantitative PCR assays were conducted with 384-well plates

(Applied Biosystems) using the standard comparative computed tomography (CT) procedure performed at OSHU Gene Profiling Shared Resource using a QuantStudio 12K Flex real-time instrument. A panel of genes were selected for qRT-PCR based on previous publications to examine oxidative stress (including *Sod1*, *Sod2*, *Nrf2*, *Nos2*, *Ho1*, *Gsr*, *Gpx1*, and *G6pd*) (Sawyer 2011; Vatner et al. 2015), inflammation (*Tnf*, *Tlr9*, *Tlr4*, *Nlrp3*, *Mcp1*, *Il6*, *Il1b*, and *Ifng*) (Castro-Jorge et al. 2017; Kamo et al. 2013), fibrosis (*Vim*, *Tgfb1*, *S100a4*, *Col1a1*, and *Acta2*) (Kayalar et al. 2020; Ning et al. 2018; Travers et al. 2016), and aging (*Myh6, Myh7, Atp2a2, Adcy5, Ercc1, Igf1r*) (Goldfarbmuren et al. 2020; Mao et al. 2018; Pandya et al. 2006; Yan et al. 2007) pathways in the heart and lung tissues. All primers were designed using Real-time qPCR assay tool and produced by Integrated DNA Technologies, Inc. (O'Leary et al. 2016). Sequence of forward and reverse primers are provided in Table S2. Relative mRNA expression was detected using the ΔΔCT method as described previously (Rao et al. 2019) and normalized to the mean of reference genes *beta-actin* or *hypoxanthine phosphoribosyltransferase* (*Hprt*) (Svingen et al. 2015) in the lung and heart tissue, respectively. Fold difference was used to compare the expression of target genes in the TRAP group with that in FA group.

Histology and Image Analysis

To evaluate fibrosis in the heart, OCT-embedded frozen heart tissue samples (middle one-third) were transversely sectioned at 10 μm using a cryostat (Leica), adhered to charged slides (Fisher Scientific), and kept at −20°C. Samples were then fixed in 10% formalin (Sigma-Aldrich) post sectioning. Collagen, muscle fiber, and nuclei of all specimens were stained using Thermo Scientific™ Richard-Allan Scientific™ Gömöri Trichrome (Blue Collagen) Kit following the manufacturer's provided protocol. Samples were mounted using aqueous mounting media and imaged using the Keyence BZ-X700 all-in-one fluorescence microscope using bright field at 10 × objective magnification standard settings (Keyence). Three sections 200 μm apart per tissue block were used for imaging. Five fields per section were randomly selected for collagen positive area analysis. Images were analyzed by two independent investigators who were blinded to the group information. ImageJ (version 1.53, National Institute of Health) software was used to determine the positive blue area as positive collagen accumulation, as previously described (Oh et al. 2011; Rao et al. 2014).

Cytokine Analysis

Plasma cytokines were measured using rat Multi-Analyte ELISArray kits (Qiagen) that include 12 cytokines: Interleukin 1 alpha (IL-1α), Interleukin 1 beta (IL-1β) Interleukin 2, 4, 6, 10, 12 and 13 (IL-2, IL-4, IL-6, IL-10, IL-12, IL-13), Interferon gamma (IFN-γ), Tumor necrosis factor alpha (TNF-α), granulocyte-macrophage colony-stimulating factor (GM-CSF), and regulated on activation, normal T cell expressed and secreted (RANTES) (Qiagen). Each plate measures six samples, one positive control, and one negative control. Absorbance was measured at 450 nm and 570 nm using a CLARIOstar® microplate reader (BMG Labtech).

Flow Cytometry

As the largest lymphoid organ in the body and the main filter for bloodborne antigens and inflammatory mediators, the spleen was used for the detection of systemic inflammatory status by measuring levels of macrophages and T cells in spleen tissue using flow cytometry. In brief, single cell suspensions isolated from the spleen tissue were stained with the following antibodies at 4°C for 30 min: Pacific Blue™ anti-rat Antibody CD45 as immune cell marker, Mouse anti-Rat CD68 Alexa Fluor® 700 (Bio-Rad) Antibody as a pan-macrophage marker, APC anti-rat CD163 Antibody as M2 macrophage marker, PE anti-rat CD80 Antibody as M1 macrophage Marker for macrophage analysis; FITC anti-rat CD62L Antibody and APC anti-rat CD4 Antibody and PE anti-rat CD3 Antibody were used for T-cell analysis. All antibodies except CD68 were purchased from BioLegend. Zombie Aqua™ Fixable Viability Kit (BioLegend) was used for viability testing. After washes, the samples were analyzed on a CytoFlex Flow cytometer (Beckman). FlowJo software (version 10.7, FlowJo) was used for the data analysis.

Statistical Analysis

Data are expressed as mean ± standard error of the mean (SEM) unless otherwise noted. Two-way analysis of variance (ANOVA) followed by Sidak's multiple comparisons test or Student's *t*-test was used to compare the means among FA and TRAP in both female and male rats, using GraphPad Prism software (version 7; GraphPad Software Inc). Statistically significant values were considered at $p < 0.05$.

Results

Exposure Design, Particles Concentration, and Characterization

Both female and male rats were bred at UC Davis. At the age of 28 d, the 24 rats (12 males and 12 females) were randomly divided into two groups/sex and exposed to traffic-related air pollution (TRAP) or filtered air (FA) for 24 h/d (6 male and 6 female rats per group), 7 d/wk, for a total of 14 months in an exposure facility adjacent to a heavily trafficked tunnel in Northern California. Air was collected from above the eastbound exit of the tunnel bores continuously without any modification for the TRAP group, whereas ambient air was drawn from surrounding the facility and filtered for the FA group. Concentrations of $PM_{2.5}$ in $\mu g/m^3$ during the continuous 14 months of exposure period were calculated using a gravimetric method. The average concentration of $PM_{2.5}$ during exposure was $11 \pm 7.4\ \mu g/m^3$ in TRAP group vs. $2.4 \pm 1.7\ \mu g/m^3$ in FA group as determined by gravimetric analysis using IMPROVE samplers ($n = 112$). Day-of-week averages of $PM_{2.5}$ and total suspended particle (TSP) concentrations in the TRAP group over the final 3-month period are illustrated in Figure 1A. Overall, $PM_{2.5}$ made up over half of the total suspended particles [57% ± 10 % for mean ± standard error of the mean (SEM)] mass concentration per $\mu g/m^3$. Both crustal elements (sodium, magnesium, aluminum, silicon, sulfur, chlorine, potassium, calcium, iron, and barium) and traffic related metals (titanium, chromium, manganese, copper, zinc, bromine, strontium, zirconium, tin, and antimony) were substantially higher in the mass fraction of $PM_{2.5}$ in comparison with FA in Figure 1B. Carbon mass concentration was also higher in $PM_{2.5}$ of TRAP in comparison with FA (Figure S2).

Body Weight and Tissue Weights in Male and Female Rats after 14-Month Exposure to TRAP

At the end of exposure, whole body, lung, heart, and spleen of all rats were weighed, shown in Figure 2. There was a significant difference in body weight between FA-exposed and TRAP-exposed male rats (463.5 ± 13.0 vs. 501 ± 12.3 g, $p = 0.02$; FA vs. TRAP) but not in the female rats (258.6 ± 5.4 vs. 273.3 ± 5.8 g, $p = 0.51$; FA vs. TRAP) (Figure 2A). To compare the tissue weights between FA and TRAP groups, tissue weights were normalized by body weight for each individual rat. Female rats had higher tissue to body weight ratios ($p < 0.001$) in the lung (Figure 2B) and heart (Figure 2C), and lower spleen to body mass ratio ($p < 0.001$;

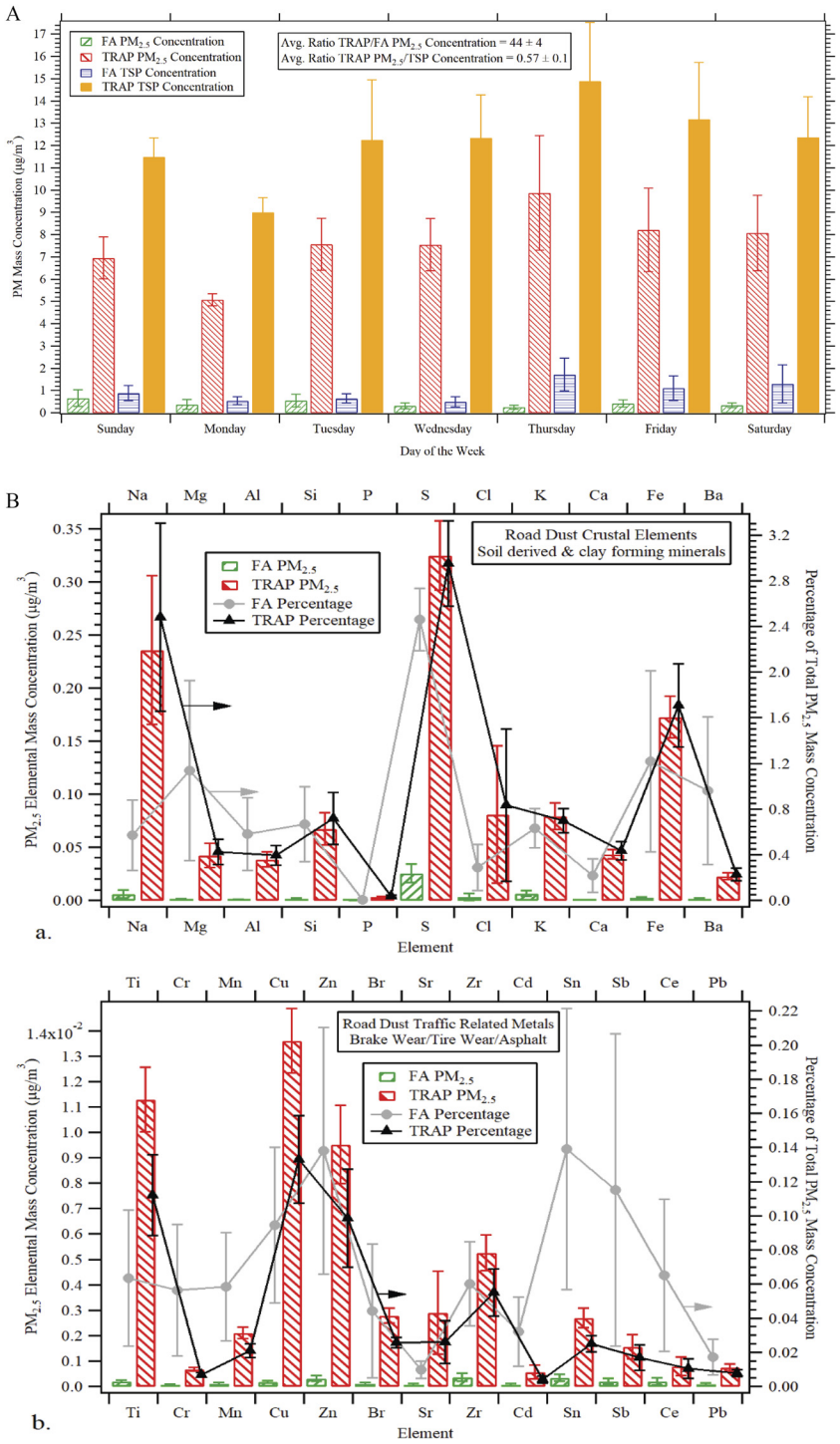

Figure 1. Average $PM_{2.5}$ concentrations and crustal or traffic related metals in the mass fraction of $PM_{2.5}$. (A) Daily measurements of filters were collected directly upstream of exposure chambers at the Facility for Roadway Air Pollution Exposure (FRAPE) for a total of 3 months prior to the 14-month study end date. Averages of PM mass concentrations were determined via gravimetric analysis in accordance with the Interagency Monitoring of Protected Visual Environments (IMPROVE). The weekly average ratio of TRAP/FA $PM_{2.5}$ concentration was 44 ± 4. The TRAP ratio of $PM_{2.5}$ TSP was 0.57 ± 0.1. $n = 4$ for each data point (TRAP TSP, TRAP $PM_{2.5}$, FA TSP, and FA $PM_{2.5}$) on each day of the week (Sunday–Saturday). (B) 24-h average concentrations of crustal elements that derived from soil and other clay forming minerals and traffic related metals that derived from multiple sources including asphalt, brake, and tire wear measured by X-ray fluorescence elemental analysis over the last 3 months of exposure. Left Axis: Elemental mass concentration of $PM_{2.5}$ in $\mu g/m^3$; Right Axis: average percentage of total $PM_{2.5}$ concentration. $n = 10$. The exact mean and SEM values for data presented here can be found in Tables S3–S4. Note: FA, filtered air; PM, particulate matter; SEM, standard error of the mean; TRAP, traffic-related air pollution; TSP, total suspended particle.

Figure 2D) compared with male rats in both FA and TRAP cohorts. However, there were no differences in normalized tissue weights between the FA and TRAP groups, suggesting that TRAP exposure did not affect the weights of lung, heart, and spleen (Figure 2B–D).

TRAP Deposition in the Lungs of Rats after Exposure

After exposure, black nodules were observed in the lung biopsy of animals exposed to TRAP in both female (Figure 3A, b and c) and male rats (Figure 3A, e and f) compared with FA exposed rats

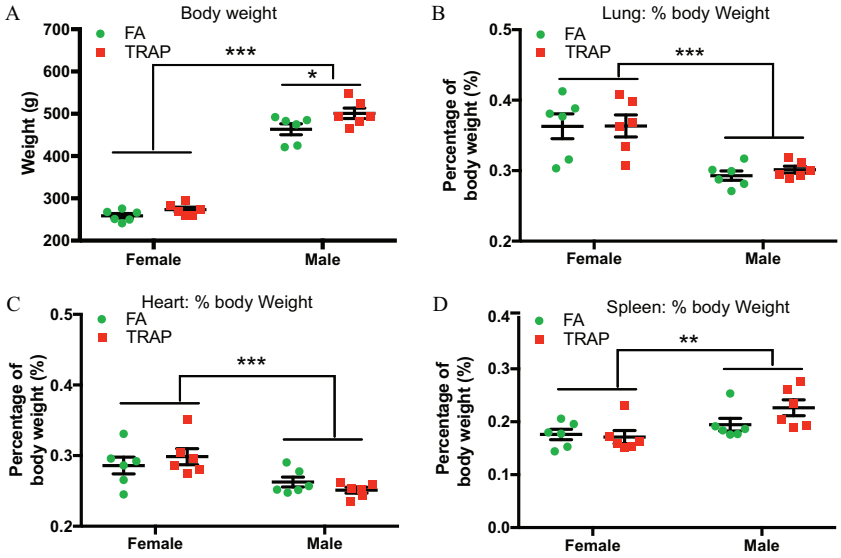

Figure 2. Comparison of body weight and normalized tissue weights in both female and male rats exposed to FA or TRAP. After 14 months of exposure to FA or TRAP, body weights (A), percentage of body weight for lung tissue (B), heart tissue (C), and spleen tissue (D) were measured in both male and female rats. Two-way analysis of variance (ANOVA) followed by Sidak's multiple comparisons test was used for statistical analysis. Mean ± SEM; $n = 6$. The exact mean and SEM values for data presented here can be found in Table S5. Note: FA, filtered air; SEM, standard error of the mean; TRAP, traffic-related air pollution. $^{*}p < 0.05$, $^{**}p < 0.01$, $^{***}p < 0.001$.

(Figure 3A, a and d). The area of nodules normalized by pleural area was then measured independently in all the groups using ImageJ (version 1.53, National Institute of Health) software by two investigators who were blinded to group information. Both female rats ($0.03\% \pm 0.01\%$ vs. $0.51\% \pm 0.08\%$, $p < 0.01$; FA vs. TRAP) and male rats ($0.01\% \pm 0.02\%$ vs. $0.47\% \pm 0.19\%$, $p < 0.01$; FA vs. TRAP) exhibited a significant higher black pigment/pleural area percentage in the lung tissues (Figure 3B).

Elemental Analysis of Lung Tissues

Next, lung tissue was digested for the detection of 65 elements via semiquantitative analysis by ICP-MS. Compared with FA group, TRAP-exposed lung tissue had a significant ($p < 0.05$) higher concentration of carbon (Figure 4A), magnesium (Figure 4C), phosphorus (Figure 4D), sulfur (Figure 4E), chromium (Figure 4F), iron (Figure 4G), nickel (Figure 4H) and bromium (Figure 4I) in the female, but not in the male rats. In contrast, a significantly higher amount of nitrogen was discovered only in the male lung tissue (Figure 4B). The other elements in the 65-element panel we tested were either nonsignificant or undetectable (Table S1).

Oxidative Stress and Inflammation Markers in Lung Tissues after TRAP Exposure

To examine the effect of TRAP exposure on oxidative stress and inflammation in the lung tissue, a panel of oxidative stress and inflammation related genes were examined by quantitative real-time PCR (qRT-PCR). The main genes of the antioxidant network include the superoxide dismutases (*Sod*), the glutathione peroxidases (*Gpx*), nuclear factor erythroid 2-related factor 2 (*Nrf2*), glucose-6-phosphate dehydrogenase (*G6pd*), and heme oxygenase-1 (*Ho1*) (Han et al. 2008). After 14 months of TRAP exposure, *Nrf2* and *Sod2*'s gene expression was significantly lower in the lung tissue of female rats only (Figure 5A). *Ho1*'s gene expression was higher in the lung tissue of male rats (Figure 5A). Major inflammatory cytokines and chemokines such as interferon gamma (*IFN-γ*), toll-like receptors (TLRs), interleukins (IL-6 and

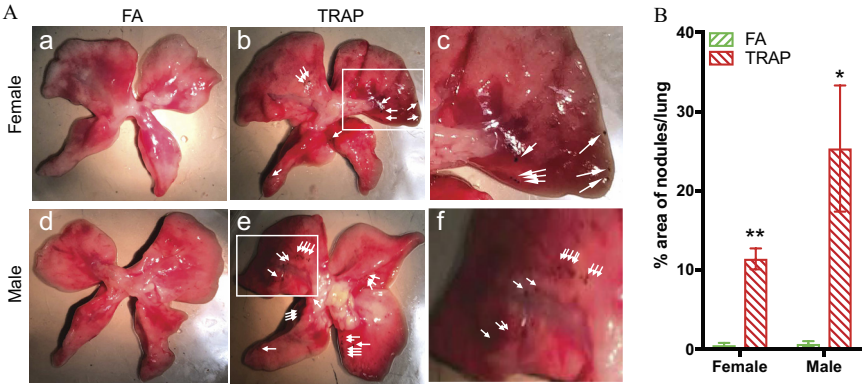

Figure 3. Macroscopic view of black nodules in the lungs after chronic exposure. (A) Representative lung images of FA-exposed female rats (a), TRAP-exposed female rats (b), FA-exposed male rats (d), and TRAP-exposed male rats (e) were selected; (c) and (f) are enlarged images of the white rectangle in figure (b) and (e), respectively. White arrowheads show black nodules found on surface of lung tissues. (B) Statistical analysis was shown in the bar graph. Two-way analysis of variance (ANOVA) followed by Sidak's multiple comparisons test was used for statistical analysis. Mean ± SEM; $n = 6$ The exact mean and SEM values for data presented here can be found in Table S6. Note: FA, filtered air; SEM, standard error of the mean; TRAP, traffic-related air pollution. $^{*}p < 0.05$ $^{**}p < 0.01$.

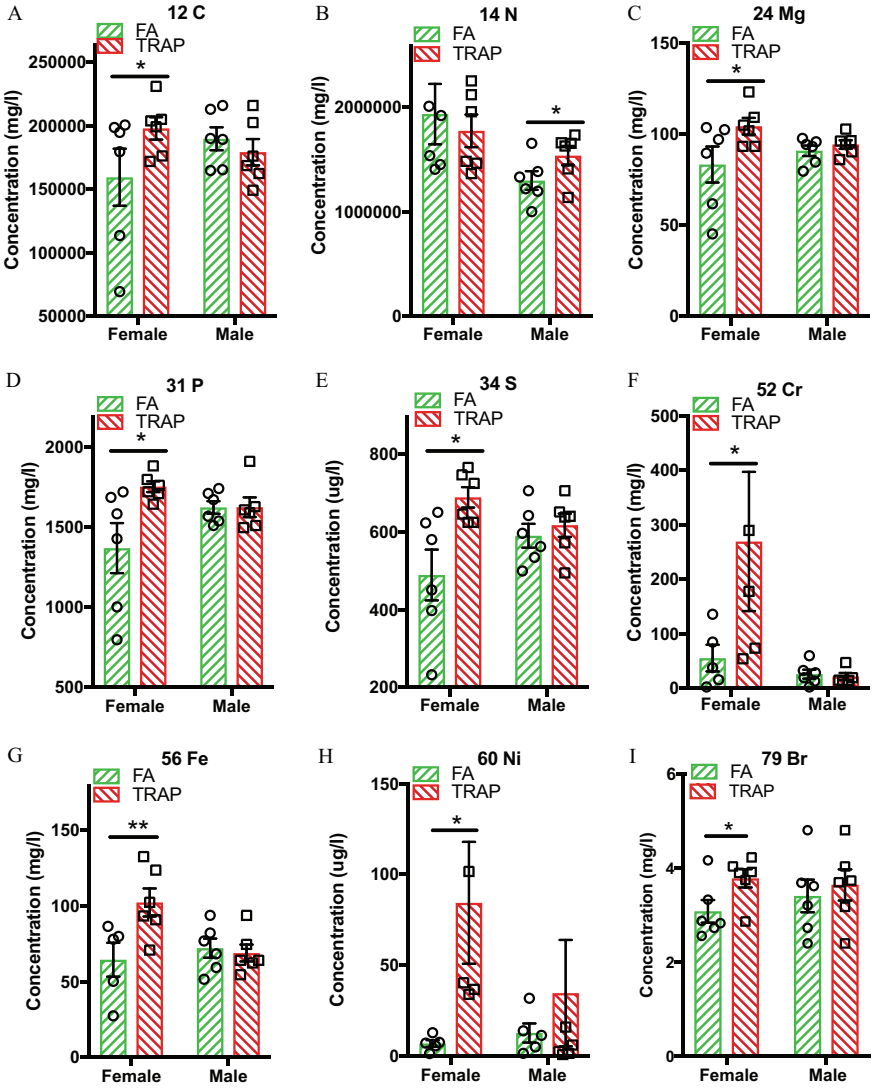

Figure 4. Elemental analysis in the lung tissues after exposure. A total of 65 elements, including carbon, nitrogen, phosphorus, sulfur, chromium, iron, and nickel, were measured in the lungs of FA- and TRAP-exposed rats. A detailed summary of all 65 element levels can be found in Table S1. (A) Carbon levels in lung tissue in mg/L. (B) Nitrogen levels in lung tissue in mg/L. (C) Magnesium levels in lung tissue in mg/L. (D) Phosphorus levels in lung tissue in mg/L. (E) Sulfur levels in lung tissue in mg/L. (F) Chromium levels in lung tissue in μg/L. (G) Iron in lung tissue in μg/L. (H) Nickel in lung tissue in μg/L. (I) Bromine in lung tissue in μg/L. Two-way analysis of variance (ANOVA) followed by Sidak's multiple comparisons test was used for statistical analysis. Mean ± SEM; $n = 6$. The exact mean and SEM values for data presented here can be found in Table S1. Note: FA, filtered air; SEM, standard error of the mean; TRAP, traffic-related air pollution. $^{*}p < 0.05$.

IL-1β), and monocyte chemoattractant protein-1 (MCP-1) were also examined for inflammation in the lung tissue after exposure. Surprisingly, no significant difference of inflammatory gene expression was observed after exposure to TRAP in both male and female rats (Figure 5B). Overall, there were minimal changes in tested genes in both oxidative stress and inflammation pathway in the lung tissue after exposure. Relative gene expression and *p*-value of each gene in the lung tissues of both male and female rats exposed to FA or TRAP are summarized in Table S7.

TRAP-Induced Sex-Specific Responses in the Heart Tissue

In addition to oxidative stress and inflammatory genes, both fibrosis and aging-related genes were evaluated in the heart via qRT-PCR (Figure 6 and Table S8). As shown in Figure 6A, glutathione-disulfide reductase (*Gsr*), a crucial component of cellular antioxidant defense via free radical uptake and xenobiotic metabolism,(Deponte 2013) was significantly higher in females after exposure. In contrast, *Ho1*, an important antioxidant implicated in protection against atherogenesis (Araujo et al. 2012), was significantly higher in male hearts. No statistically significant difference was observed in other genes evaluated in both females and males, though there was a trend of higher gene expression of *G6pd* and *Nrf2* in females (Figure 6A).

Inflammation related genes were higher in both male and female hearts after exposure (Figure 6B). These genes included significant higher expression of cytokines interferon gamma (IFN-γ), IL-6, and tumor necrosis factor alpha (TNF-α). Expression of *Ifng* was higher in both male and female hearts. IL-6 and TNF-α were higher in female hearts only after TRAP exposure. Both females and males had a higher expression of NLR family pyrin domain containing 3 (*Nlrp3*) and Toll-like receptor 4 (*Tlr4*). Although not statistically significant, there was a trend for genes of *Mcp1* and *Tnf*α to be higher by TRAP exposure in male hearts.

The expression of fibrosis related genes was then examined in the heart (Figure 6C) and lung (Figure S3) tissues. No difference

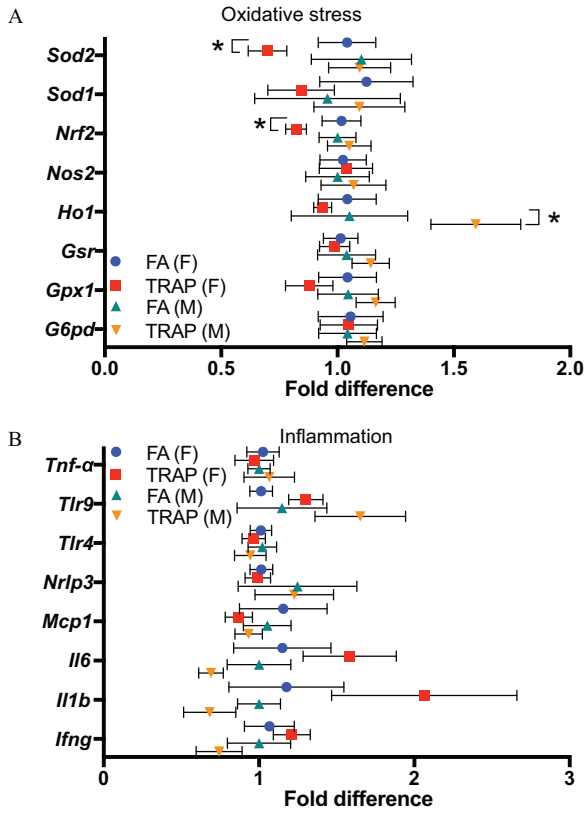

Figure 5. Expression of oxidative stress and inflammation-related genes were examined in the lung tissues by qRT-PCR. (A) Fold difference of oxidative stress-related genes in lungs from both female and male rats exposed to FA or TRAP. (B) Fold difference of inflammatory genes in lungs from both female and male rats exposed to FA or TRAP. Fold differences in gene expression were calculated by delta delta CT (cycle threshold) method ($2^{-\Delta\Delta CT}$). All gene expressions were normalized by expression of housekeeping gene beta-actin and FA group was used as a reference group when calculating the ΔΔCT values. The formulas are: ΔCT = CT (gene of interest) − CT (*beta-actin*); ΔΔCT = ΔCT (TRAP) − ΔCT (average of FA); Fold gene expression = $2^{\wedge -\Delta\Delta Ct}$. Two-way analysis of variance (ANOVA) followed by Sidak's multiple comparisons test was used for statistical analysis. Mean ± SEM; $n = 6$ The exact mean and SEM values for data presented here can be found in Table S7. Note: FA, filtered air; SEM, standard error of the mean; TRAP, traffic-related air pollution. $^{*}p < 0.05$.

was observed in the male hearts, whereas most of the tested genes were higher in the female hearts after TRAP exposure. Gene expression of smooth muscle aortic alpha-actin (*Acta2*), collagen, type I, alpha 1 (*Col1a1*), S100 calcium-binding protein A4 (*S100a4*), transforming growth factor-beta (*Tgfb1*) were higher only in female rats. Type III intermediate filament protein (*Vim*) was not significantly different, but there was a trend for it to be higher in TRAP-exposed animals ($p = 0.06$). In contrast, the expression of fibrosis related genes in the lungs was not significantly different between the TRAP and FA groups in the lungs of TRAP-exposed females, whereas *Col1a1* was higher in the lungs of TRAP-exposed males (Figure S3).

Both insulin-like growth factor-1 (*Igf1r*) and excision repair cross-complementation group 1 (*Ercc1*) were significantly higher in female, but not in male, hearts following TRAP exposure, as shown in Figure 6D.

Collagen Accumulation in the Heart of TRAP-Exposed Females

Because qRT-PCR results showed a higher level of fibrosis-related gene expression in the females only, we measured collagen accumulation in the heart using Gömöri Trichrome staining. As shown in Figure 7A, the collagen fibers were stained as blue to differentiate from the heart muscle, which was stained as red. The collagen positive area was then calculated and normalized by tissue area to compare the collagen accumulation in the hearts in Figure 7B. In concordance with the qRT-PCR result, only females displayed significantly more collagen accumulation (mean ± SEM: 8.26% ± 0.58% vs. 14.27% ± 1.35%, $p < 0.01$; FA vs. TRAP) in the heart in response to TRAP exposure.

Systemic Immune Responses in the Female and Male Rats after TRAP Exposure

To investigate the effect of TRAP exposure on systemic inflammation, 12 cytokines/chemokines in plasma were measured via enzyme-linked immunosorbent assay. We also used flow cytometry to measure inflammatory cell populations in the spleen, the largest secondary lymphoid organ. Inflammatory cytokines in circulation are important mediators that induce the systemic inflammation in air pollution exposure. After 14 months of TRAP exposure, the levels of proinflammatory cytokines TNF-α, IFN-γ, and interleukin 1α(IL-1α) were higher in the plasma of female rats, whereas there was a higher level of proinflammatory cytokine IL-1β and a lower expression of anti-inflammatory cytokine IL-10 in the male rats (Figure 8A and 8B).

Flow cytometry analysis of the spleen in males (Figure 8C and 8D) showed a significantly higher levels of M1 macrophages and a significantly lower level of M2 macrophages after TRAP exposure. T-cell populations were not significantly different in males or females (Figure 8E). In contrast, neither M1 nor M2 macrophages were higher in TRAP-exposed females (Figure 8C and 8D). Males exhibited a significant enhanced overall innate immune response in comparison with females as evidenced by the significantly higher M1 macrophage populations.

Discussion

Humans are increasingly exposed chronically to anthropomorphic sources of air pollution worldwide (Shaddick et al. 2020). TRAP is a dynamic pollutant whose concentration, source, and components can vary drastically over the course of a single day (Manning et al. 2018; Zhang and Batterman 2013). Examination of the health effects of TRAP exposure, especially chronic exposures, is important and biologically relevant because people frequently commute and live near highways and freeways. Tunnel exposure represents direct traffic exposure for people commuting frequently. It has also been used as a well-recognized model to mimic near roadway residential exposure (Kuykendall et al. 2009), although the components and concentrations of pollutants in residential areas near roadways vary depending on the traffic load, topography, meteorology, and distance from the roadway. This study used a real-world 24 h TRAP exposure based on actual traffic patterns and emissions. Animals were exposed to a biologically relevant mixture, frequency, and concentration of TRAP, providing a better model to begin evaluating the risk TRAP has on individuals who live near highways and those who commute frequently.

There have been several studies using tunnel traffic as a model to assess the characterization of traffic pollutants and their health effects, with average concentrations ranging from 24.9 to 793 $\mu g/m^3$ for $PM_{2.5}$ (Ding et al. 2016; Emmerechts et al. 2012), from 93.8 to 1,221 $\mu g/m^3$ for PM_{10} (Ding et al. 2016; Emmerechts et al. 2012), from 230 to 313 (Larsson et al. 2010) $\mu g/m^3$ for NO_2 (Larsson et al. 2007, 2010; Svartengren et al. 2000), and from 711 to 874 $\mu g/m^3$ for NO (Larsson et al. 2007, 2010), depending on the location of these facilities. The effect of TRAP exposure largely depends on the location, concentration, and exposure duration.

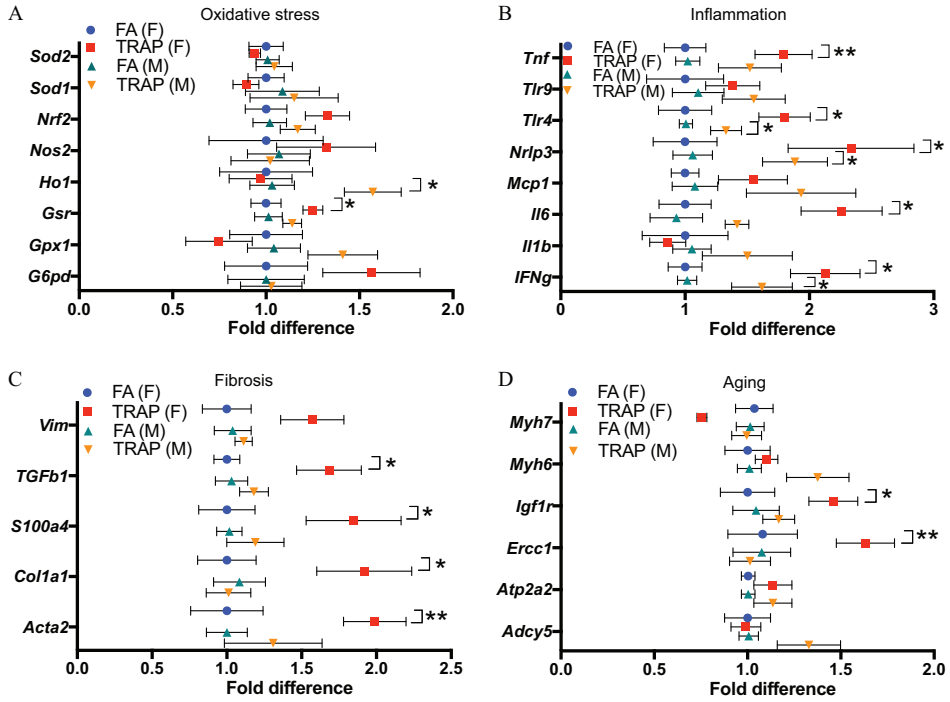

Figure 6. Expression of genes mediating oxidative stress, inflammation, fibrosis, and aging in female and male hearts of rats exposed to FA or TRAP. (A) Fold difference of oxidative stress–related genes in hearts of both female and male rats exposed to FA or TRAP. (B) Fold difference of inflammatory genes in hearts of both female and male rats exposed to FA or TRAP. (C) Fold difference of fibrosis-related genes in hearts of both female and male rats exposed to FA or TRAP. (D) Fold difference of aging-related genes in hearts of both female and male rats exposed to FA or TRAP. Fold differences in gene expression were calculated by delta delta cycle threshold (CT) method ($2^{-\Delta\Delta CT}$). All gene expressions were normalized by expression of housekeeping gene Hrpt and FA group was used as a reference group when calculating the ΔΔCT values. The formulas are: ΔCT = CT (gene of interest) − CT (*Hrpt*); ΔΔCT = ΔCT (TRAP) − ΔCT (average of FA); Fold gene expression = $2^{\wedge -\Delta\Delta Ct}$. Two-way analysis of variance (ANOVA) followed by Sidak's multiple comparisons test was used for statistical analysis. Mean ± SEM; $n = 6$. The exact mean and SEM values for data presented here can be found in Table S8. Note: FA, filtered air; SEM, standard error of the mean; TRAP, traffic-related air pollution. $^{*}p < 0.05$ $^{**}p < 0.01$.

Enhanced asthmatic reactions were observed after acute exposure (30 min) to tunnel air in Stockholm, Sweden (Svartengren et al. 2000). Similarly, Larsson et al. observed more asthmatic symptoms (Larsson et al. 2010) and a greater airway inflammatory response (Larsson et al. 2007) in a small group of individuals exposed to tunnel air acutely for 30 min to 2 h. In contrast, no overt pulmonary or systemic inflammation were observed when Fisher rats were continuously exposed to roadside and diesel engine exhaust particles for 25 to 28 d (Gerlofs-Nijland et al. 2010). However, long-term exposure at a low concentration and sex effects on cardiopulmonary and immune system have not been previously examined. Previous animal studies that have examined TRAP exposure have primarily been conducted on male animals. Male physiology is widely understood to be different from female physiology regarding absorption, distribution, metabolism, and elimination. This distinction is critical because mounting evidence indicates that sex differences may mediate different diseases and outcomes after exposure to various pollutants (Gochfeld 2017; Vahter et al. 2007). Indeed, we found different pathophysiological responses to TRAP exposure between male and female rats in the current study. Research has shown that, overall, female adults are more at risk of asthma (de Marco et al. 2000) due to lung capacity, airway size, flow rate, and other factors. In our study, we found that levels of eight metal elements such as iron and magnesium from fossil fuel combustion and tires were higher in the lungs from TRAP-exposed females, whereas levels of only one element were higher in the TRAP-exposed male lungs. Female rats were also more susceptible to TRAP-induced cardiac fibrosis, oxidative stress, inflammation, and aging. The current study has also revealed that female rats had a greater organ to body weight percentage than males in regard to both lungs and hearts, illustrating a key difference in physiology based on sex (Clougherty 2010). Adolescent male mice have been shown to have more visceral fat after exposure to $PM_{2.5}$ (Xu et al. 2010). Although this study did not examine visceral fat of animals, male rats in our study did have a significantly higher body weight after TRAP exposure, unlike females, thus contributing further evidence that TRAP may promote obesity in males.

In our study, black nodules were found in lungs of TRAP-exposed rats. This observation is consistent with the finding that pollutant deposition was found in the pleural surface of lungs from individuals with chronic traffic exposure in Sao Paulo, Brazil (Takano et al. 2019), suggesting that the black nodules found in our study were depositions of insoluble TRAP constituents from the inhaled air. Although it is important to examine the elemental health impacts to gain insight into how each component may contribute to disease, the chemical constituents of TRAP are complex (Lough et al. 2005), and analyzing single components will miss potential synergistic effects. We thus took the TRAP approach but acknowledge that this study could not distinguish the biological mechanisms of each pollutant found in TRAP. Because studies have found toxicological differences between male and female uptake of various elements and metals, it is important to evaluate uptake and health outcomes based on sex (Wilbur et al. 2012). One important example is that females freely uptake divalent transition metal ions and other metals, especially during reproductive age due to anemia (Lee and Kim 2014). This uptake is particularly observed with iron, which has been found to catalyze reactive species leading to atherogenesis (Alissa and Ferns 2011). In this study, metals such as iron and magnesium from both fossil fuel combustion and from tires on roadways (Grigoratos and Martini 2015; Vouk and Piver 1983; Zhou et al. 2014) were found to be higher in female, but not male, lung tissue after TRAP exposure,

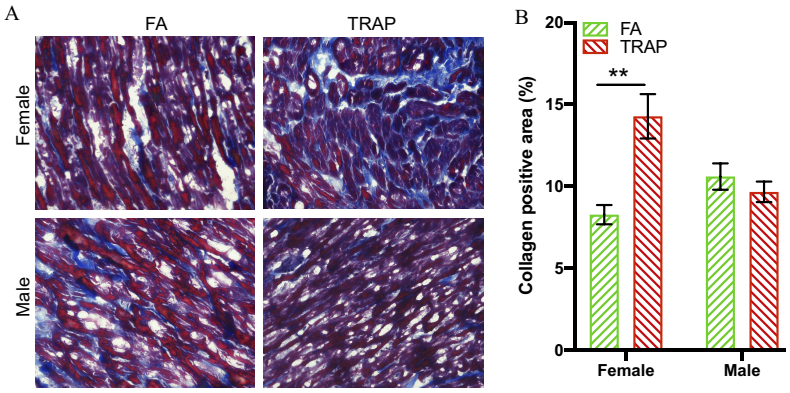

Figure 7. Gömöri trichrome staining in hearts from rats exposed to FA or TRAP. (A) Representative 40× objective bright-field images show distribution of collagen (blue) in heart tissue of FA and TRAP-exposed rats. Muscle fibers were stained as red color. (B) Statistical analysis of collagen accumulation in heart normalized by tissue area. Two-way analysis of variance (ANOVA) followed by Sidak's multiple comparisons test was used for statistical analysis. Mean ± SEM; $n = 6$. The exact mean and SEM values for data presented here can be found in Table S9. Note: FA, filtered air; SEM, standard error of the mean; TRAP, traffic-related air pollution. $^{**}p < 0.01$.

despite the deposition of insoluble TRAP constituents (black nodules) being similar in TRAP-exposed males and females. These data suggest that females are more efficient in taking up various elements and metals, which may have contributed to the oxidative stress and inflammation found in female heart tissue. Additionally, chromium, which is generated from fossil fuel combustion, was found to be only slightly higher in TRAP but was found to be significantly higher in female lung tissue post exposure. Despite a slightly higher level of chromium in TRAP in comparison with the FA group, one study showed that females were more sensitive to inhalation of chromium than males (Wilbur et al. 2012) and may have contributed to cardiac fibrosis. In this study, high levels of nickel were found in female lung tissue. This information is critical because research has correlated high levels of nickel, found in TRAP from fossil fuel combustion, with adverse health impacts in humans (Figueroa et al. 2006) and in an animal study, which showed that a high level of nickel was associated with changes in heart rate and variability (Lippmann et al. 2006).

Despite the deposition and elemental analysis, mRNA levels of oxidative stress and inflammation-related genes were relatively unchanged. RT qPCR analysis showed a lower expression in *Nrf2*, which controls expression of antioxidant response elements (ARE) to regulate resistance to free radicals/oxidants (Nguyen et al. 2009), and *Sod2*, which binds to the superoxide and converts it to hydrogen peroxide and oxygen (Sawyer 2011), in female rats. Lower expression of these critical antioxidant related genes can lead to enhanced systemic oxidative stress. Our findings that there were less or minimal differences in oxidative stress or inflammation-related genes may be explained by the real-world TRAP exposure level in this region of California, which was at or below the National Ambient Air Quality Standard of 12 $\mu g/m^3$ (U.S. EPA 2013) in marked contrast to many preclinical studies of air pollution. The average $PM_{2.5}$ concentration in our study was 12 $\mu g/m^3$, whereas most of the previous studies used concentrated ambient air PM or diesel exhaust particulate, which are usually 6- to 10-fold higher (Rao et al. 2019; Wold et al. 2012; Xu et al. 2010). These results suggest that the toxicity of TRAP might be dose-dependent, and exposure levels as low as 12 $\mu g/m^3$ may still cause systemic oxidative stress and inflammation. Another possible reason for the low levels of oxidative stress and inflammation found in the current study is that the animals were exposed for 14 months, and exposure to chronic, constant, low level of TRAP may either trigger compensatory mechanisms or exhaust the oxidative stress/inflammatory response.

Cardiac remodeling characterized by fibrosis is one of the major pathological mechanisms for cardiac dysfunction (Wold et al. 2012). Concentrated ambient $PM_{2.5}$ exposure was associated with enhanced cardiac fibrosis and cardiac dysfunction characterized by decreased fractional shortening and reduced diastolic function in mice (Wold et al. 2012). In a mouse study, it was shown that $PM_{2.5}$ exposure enhanced angiotensin II-induced cardiac hypertrophy and collagen deposition by activating cardiac and vascular RhoA/Rho-kinase (Ying et al. 2009), a pathway closely related to oxidative stress (Sun et al. 2008). In those previous studies, animals were exposed to high concentrations of $PM_{2.5}$ (concentrated fine PM) but only male mice were used. In our study, we found that chronic exposure to real-world TRAP levels promoted cardiac fibrosis in female but not male rats. Inflammation and aging pathways have also been shown to mediate the process of fibrosis in air pollution exposure (Johannson et al. 2015). Reactive oxygen species (ROS), either directly from air pollutants such as O_3, NO_2, and certain components in $PM_{2.5}$ or endogenously generated from pollutant-elicited biological processes, may facilitate the clearance of pollutants and recovery from tissue damage in early stages. Kagan et al. demonstrated that the digestion of exogenous carbonaceous nanoparticles by macrophages requires NADPH oxidase 2 (Nox2) (Kagan et al. 2014). When the production of ROS exceeds the clearing capacity of antioxidative system, excessive ROS results in tissue damage and subsequent repairing processes, such as inflammation and tissue remodeling/fibrosis. In support of this, a recent study showed that air pollution–induced oxidative stress contributes to cardiac collagen accumulation and fibrosis. Deficiency of antioxidative *Nrf2* dramatically exacerbated air pollution-induced cardiac fibrosis and cardiac dysfunction in mice (Ge et al. 2020). In addition to oxidative stress, inflammation and telomere shortening are also important pathways mediating the adverse effects of air pollution on pulmonary fibrosis (Johannson et al. 2015). In this study, we found that the expressions of genes involved in oxidative stress (*Ho1* and *Gsr*), inflammation (*Tnf*, *Tlr4*, *Nlrp3*, *Il6*, and *Ifng*), and aging (*Igf1r* and *Ercc1*) were higher in TRAP-exposed animals, especially in females. These results indicate that oxidative stress, inflammation, and aging may play a role in TRAP-induced cardiac fibrosis.

Recent epidemiological studies indicate females exposed to TRAP present more adverse health effects than males (Clougherty 2010; Franklin et al. 2007; Kim et al. 2019; Stockfelt et al. 2017). Long-term exposure to air pollution has been linked to a higher incidence of cardiovascular events in women (Clougherty 2010; Stockfelt et al. 2017), and our findings complement epidemiological studies because female rats exhibited more severe heart

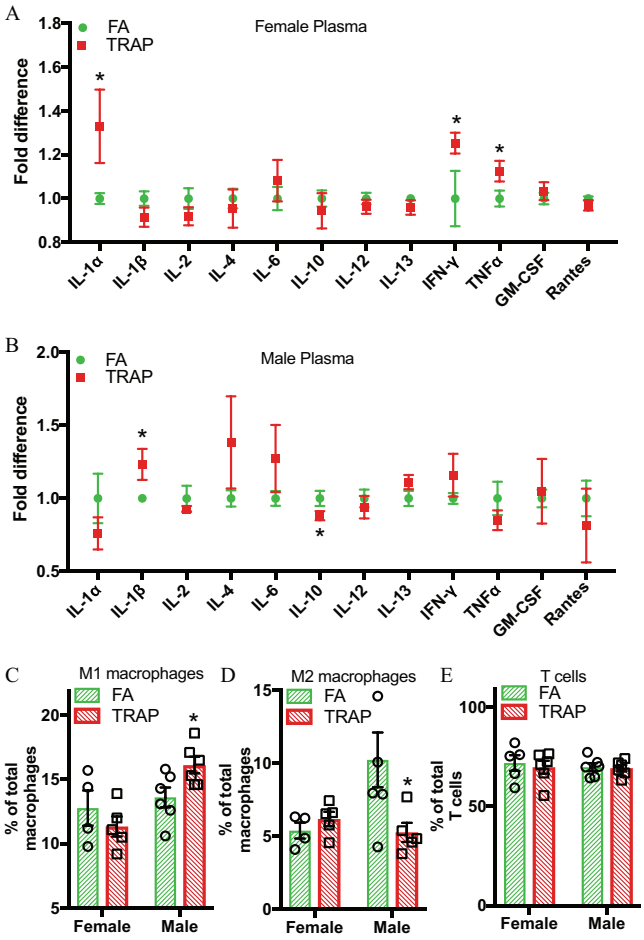

Figure 8. Systemic immune responses in both female and male rats after TRAP exposure. (A) and (B), Twelve cytokines/chemokines, including interleukins, IFNγ, TNFα, GM-CSF, and RANTES were tested in the plasma of both female (A) and male (B) rats by enzyme-linked immunosorbent assay. Comparison of fold difference (TRAP/FA) was shown in the figure. Student's *t*-test was used to compare the difference between FA and TRAP group for each cytokine in both female and male rats. (C–E) Cells were isolated from spleen, stained with macrophage and T-cell markers, and detected by flow cytometry. Percentage of $CD45^+CD68^+CD80^+$ M1 (classically activated macrophages), $CD45^+CD68^+CD163^+$ M2 (alternatively activated macrophages), and $CD3^+CD4^+CD62L^-$ T cells (activated T cells) in total macrophages and T cells were presented in both female and males. Two-way analysis of variance (ANOVA) followed by Sidak's multiple comparisons test was used for statistical analysis. Mean ± SEM; $n = 4-6$. The exact mean and SEM values for data presented here can be found in Tables S10–S11. Note: FA, filtered air; SEM, standard error of the mean; TRAP, traffic-related air pollution. $^*p < 0.05$.

pathology following TRAP exposure. Female rats had significantly higher cytokine and innate immune responses after exposure to TRAP indicating higher levels of inflammation in heart tissue. Cardiac fibrosis in females exposed to TRAP was further confirmed via trichrome staining showing more collagen deposition, which usually is a consequence of chronic insult to the myocardium (Hinderer and Schenke-Layland 2019). These results were in contrast to those from the males, which showed no difference in expression of genes for fibrogenesis or collagen deposition. This difference may be because the antioxidant *Ho1* was higher in male heart tissues, which may have provided a cardio-protective effect (Wang et al. 2010) against TRAP-induced cardiac injury. Consistent with this suggestion, anti-inflammatory cytokine IL-10 was higher in the plasma of male rats after TRAP exposure. IL-10 has been shown to have an immunosuppressive effect inhibiting the synthesis of both IFN-γ and TNFα (Cyktor and Turner 2011), both of which were higher in female plasma but not in male rats. These results indicate that males may have better compensatory ability against TRAP-induced oxidative and inflammatory response. In addition, low expressions of *Tnf* and *Il6* in male heart tissues may also contribute to the gender difference in cardiac fibrosis. The expressions of *Tnf* and *Il6*, both of which are suggested to enhance fibrosis (Fielding et al. 2014; Nakahara et al. 2003; Piguet et al. 1990; Pilling et al. 2015), were higher in the heart from TRAP-exposed females, but not in males.

Evidence has shown that both innate and adaptive immune response differ due to sex differences (Ruggieri et al. 2016), which was directly observed in this study but not considered in many other animal model air pollution studies. Although our study examined the adverse effects of real-world TRAP exposure on cardiopulmonary diseases and underlying oxidative and inflammatory response, it had some limitations. First, because our system exposed animals to unmodified real-world levels of TRAP, the composition, concentration, frequency, and fluctuations found naturally in real-world TRAP make it difficult to establish causal relationships between adverse effects and specific TRAP components. For example, this study does not allow discernment of the relative health effects particle vs. gaseous pollutants. Although PM derived from vehicles is highly oxidative and toxic (Kelly 2003), the potential effect of gases such as NO_x and secondary pollutants such as sulfates and nitrates cannot be neglected. A recent epidemiologic study on 3,920 individuals free from pre-existing cardiovascular disease in the United Kingdom reported that a larger ventricular volume as measured by cardiovascular magnetic resonance imaging was associated with both $PM_{2.5}$ and NO_2 concentrations (Aung et al. 2018). In addition to PM and NO_2, increased exposure to SO_2, CO, and secondary pollutant O_3 was associated with cardiac arrhythmia and stroke (Hong et al. 2002; Xu et al. 2019). Despite its limitations on concise exploration of specific contribution of each gaseous and particulate pollutant to disease, tunnel exposure integrates the multifaceted and unique elemental makeup of TRAP that individuals are exposed to daily. A second limitation is that because this was a pilot study, the sample size was relatively small, the histopathologic assessments were limited, and cardiopulmonary function was not examined. Future studies are required to further assess sex-specific effects of chronic TRAP exposure on cardiopulmonary functions and histopathological changes. Third, specific molecular mechanisms by which TRAP results in cardiac pathological changes were not examined in this study. This aspect could be addressed by exposing specific transgenic/knockout models or using pharmacological inhibitors in the future studies. Finally, although no adverse effects related to age were observed in the control group, animals were sacrificed at 15 months of age, near the end of their biological lifespan, and therefore TRAP may have exacerbated the development of naturally progressing disease, including cardiopulmonary disease and cancer, adding another confounding variable to this study.

In conclusion, this study adds additional evidence to the growing body of epidemiological air pollution research associating females with exhibiting greater cardiopulmonary effects, particularly those exposed chronically to TRAP. Females overall may be considered a more vulnerable population regarding cardiopulmonary diseases. Examination of female-specific and sex-different mechanisms of air pollution exposure is not yet explored in many air pollution studies and should receive increased scrutiny. Future directions could evaluate the role of hormones and sex differences on air pollution toxicity and greater analysis of the constituents and whole-body effects of TRAP. These findings elucidate the need for gender- or sex-based analysis in further air pollution research, particularly about ubiquitous, real-world,

nonconcentrated, and chronic TRAP exposure, which can cause significant systemwide negative health effects.

Acknowledgments

ICP-MS measurements were performed in the OHSU Elemental Analysis Core with partial support from the National Institutes of Health (NIH) instrumentation grant S10RR025512.

This work was supported by NIH (R00 ES026241 to XR, R21 ES025570, R21 ES026515, and P30 ES023513 to P.J.L.). K.T.P. was supported by NIH-funded predoctoral training programs awarded to the University of California, Davis (UC Davis; T32 MH112507 and T32 ES007059).

The contents of this work do not necessarily represent the official views of the NIH, and the NIH does not endorse the purchase of any commercial products or services mentioned in the publication.

References

Air Quality Research Center. 2020a. UCD IMPROVE Standard Operating Procedure #301: X-Ray Fluorescence Analysis of Aerosol Deposits on PTFE Filters. UC Davis, http://vista.cira.colostate.edu/improve/wp-content/uploads/2020/07/IMPROVE-SOP-301_XRF-Analysis-of-Aerosol-Deposits-on-PTFE-Filters_2020_FINAL_signed.pdf [accessed 30 November 2020].

Air Quality Research Center. 2020b. UCD IMPROVE Standard Operating Procedure #351: Data Processing and Validation. UC Davis, http://vista.cira.colostate.edu/improve/wp-content/uploads/2020/07/IMPROVE-SOP-351_Data-Processing-and-Validation_2020_FINAL_signed.pdf [accessed 30 November 2020].

Air Quality Research Center. 2020c. UCD IMPROVE Standard Operating Procedure #251: Sample Handling. UC Davis, http://vista.cira.colostate.edu/improve/wp-content/uploads/2020/07/IMPROVE-SOP-251_Sample-Handling-2020_FINAL_signed.pdf [accessed 30 November 2020].

Alexeeff SE, Roy A, Shan J, Liu X, Messier K, Apte JS, et al. 2018. High-resolution mapping of traffic related air pollution with Google street view cars and incidence of cardiovascular events within neighborhoods in Oakland, CA. Environ Health 17(1):38, PMID: 29759065, https://doi.org/10.1186/s12940-018-0382-1.

Alissa EM, Ferns GA. 2011. Heavy metal poisoning and cardiovascular disease. J Toxicol 2011:870125, PMID: 21912545, https://doi.org/10.1155/2011/870125.

Allen JO, Mayo PR, Hughes LS, Salmon LG, Cass GR. 2001. Emissions of size-segregated aerosols from on-road vehicles in the Caldecott tunnel. Environ Sci Technol 35(21):4189–4197, https://doi.org/10.1021/es0015545.

Araujo JA, Zhang M, Yin F. 2012. Heme oxygenase-1, oxidation, inflammation, and atherosclerosis. Front Pharmacol 3:119, PMID: 22833723, https://doi.org/10.3389/fphar.2012.00119.

Aung N, Sanghvi MM, Zemrak F, Lee AM, Cooper JA, Paiva JM, et al. 2018. Association between ambient air pollution and cardiac morpho-functional phenotypes: insights from the UK Biobank population imaging study. Circulation 138(20):2175–2186, PMID: 30524134, https://doi.org/10.1161/CIRCULATIONAHA.118.034856.

Ban-Weiss GA, McLaughlin JP, Harley RA, Lunden MM, Kirchstetter TW, Kean AJ, et al. 2008. Long-term changes in emissions of nitrogen oxides and particulate matter from on-road gasoline and diesel vehicles. Atmos Environ 42(2):220–232, https://doi.org/10.1016/j.atmosenv.2007.09.049.

Bates DV. 1995. The effects of air pollution on children. Environ Health Perspect 103(suppl 6):49–53, PMID: 8549489, https://doi.org/10.2307/3432345.

Berg EL, Pedersen LR, Pride MC, Petkova SP, Patten KT, Valenzuela AE, et al. 2020. Developmental exposure to near roadway pollution produces behavioral phenotypes relevant to neurodevelopmental disorders in juvenile rats. Transl Psychiatry 10(1):289, PMID: 32807767, https://doi.org/10.1038/s41398-020-00978-0.

Bernstein JA, Alexis N, Barnes C, Bernstein IL, Nel A, Peden D, et al. 2004. Health effects of air pollution. J Allergy Clin Immunol 114(5):1116–1123, PMID: 15536419, https://doi.org/10.1016/j.jaci.2004.08.030.

Bourdrel T, Bind MA, Béjot Y, Morel O, Argacha JF. 2017. Cardiovascular effects of air pollution. Arch Cardiovasc Dis 110(11):634–642, PMID: 28735838, https://doi.org/10.1016/j.acvd.2017.05.003.

Brook RD, Franklin B, Cascio W, Hong Y, Howard G, Lipsett M, et al. 2004. Air pollution and cardiovascular disease: a statement for healthcare professionals from the expert panel on population and prevention science of the American Heart Association. Circulation 109(21):2655–2671, PMID: 15173049, https://doi.org/10.1161/01.CIR.0000128587.30041.C8.

Calderón-Garcidueñas L, Solt AC, Henríquez-Roldán C, Torres-Jardón R, Nuse B, Herritt L, et al. 2008. Long-term air pollution exposure is associated with neuroinflammation, an altered innate immune response, disruption of the blood-brain barrier, ultrafine particulate deposition, and accumulation of amyloid β-42 and α-synuclein in children and young adults. Toxicol Pathol 36(2):289–310, PMID: 18349428, https://doi.org/10.1177/0192623307313011.

Castro-Jorge LA, Pretto CD, Smith AB, Foreman O, Carnahan KE, Spindler KR. 2017. A protective role for interleukin-1 signaling during mouse adenovirus type 1-induced encephalitis. J Virol 91(4): PMID: 27903802, https://doi.org/10.1128/JVI.02106-16.

Chow JC, Watson JG, Chen LW, Chang MC, Robinson NF, Trimble D, et al. 2007. The IMPROVE_A temperature protocol for thermal/optical carbon analysis: maintaining consistency with a long-term database. J Air Waste Manag Assoc 57(9):1014–1023, PMID: 17912920, https://doi.org/10.3155/1047-3289.57.9.1014.

Clougherty JE. 2010. A growing role for gender analysis in air pollution epidemiology. Environ Health Perspect 118(2):167–176, PMID: 20123621, https://doi.org/10.1289/ehp.0900994.

Cohen AJ, Brauer M, Burnett R, Anderson HR, Frostad J, Estep K, et al. 2017. Estimates and 25-year trends of the global burden of disease attributable to ambient air pollution: an analysis of data from the Global Burden of Diseases study 2015. Lancet 389(10082):1907–1918, PMID: 28408086, https://doi.org/10.1016/S0140-6736(17)30505-6.

Cyktor JC, Turner J. 2011. Interleukin-10 and immunity against prokaryotic and eukaryotic intracellular pathogens. Infect Immun 79(8):2964–2973, PMID: 21576331, https://doi.org/10.1128/IAI.00047-11.

de Marco R, Locatelli F, Sunyer J, Burney P. 2000. Differences in incidence of reported asthma related to age in men and women. Am J Respir Crit Care Med 162(1):68–74, PMID: 10903222, https://doi.org/10.1164/ajrccm.162.1.9907008.

Deponte M. 2013. Glutathione catalysis and the reaction mechanisms of glutathione-dependent enzymes. Biochim Biophys Acta 1830(5):3217–3266, PMID: 23036594, https://doi.org/10.1016/j.bbagen.2012.09.018.

Ding R, Jin Y, Liu X, Zhu Z, Zhang Y, Wang T, et al. 2016. H3K9 acetylation change patterns in rats after exposure to traffic-related air pollution. Environ Toxicol Pharmacol 42:170–175, PMID: 26855416, https://doi.org/10.1016/j.etap.2016.01.016.

Dominici F, Wang Y, Correia AW, Ezzati M, Pope CA 3rd, Dockery DW. 2015. Chemical composition of fine particulate matter and life expectancy: in 95 US counties between 2002 and 2007. Epidemiology 26(4):556–564, PMID: 25906366, https://doi.org/10.1097/EDE.0000000000000297.

Emmerechts J, De Vooght V, Haenen S, Loyen S, Van Kerckhoven S, Hemmeryckx B, et al. 2012. Thrombogenic changes in young and old mice upon subchronic exposure to air pollution in an urban roadside tunnel. Thromb Haemost 108(4):756–768, PMID: 22872007, https://doi.org/10.1160/TH12-03-0161.

Fielding CA, Jones GW, McLoughlin RM, McLeod L, Hammond VJ, Uceda J, et al. 2014. Interleukin-6 signaling drives fibrosis in unresolved inflammation. Immunity 40(1):40–50, PMID: 24412616, https://doi.org/10.1016/j.immuni.2013.10.022.

Figueroa DA, Rodríguez-Sierra CJ, Jiménez-Velez BD. 2006. Concentrations of NI and V, other heavy metals, arsenic, elemental and organic carbon in atmospheric fine particles ($PM_{2.5}$) from Puerto Rico. Toxicol Ind Health 22(2):87–99, https://doi.org/10.1191/0748233706th247oa.

Franklin M, Zeka A, Schwartz J. 2007. Association between $PM_{2.5}$ and all-cause and specific-cause mortality in 27 US communities. J Expo Sci Environ Epidemiol 17(3):279–287, PMID: 17006435, https://doi.org/10.1038/sj.jes.7500530.

Ge C, Hu L, Lou D, Li Q, Feng J, Wu Y, et al. 2020. Nrf2 deficiency aggravates PM2.5-induced cardiomyopathy by enhancing oxidative stress, fibrosis and inflammation via RIPK3-regulated mitochondrial disorder. Aging (Albany NY) 12(6):4836–4865, PMID: 32182211, https://doi.org/10.18632/aging.102906.

Geller MD, Sardar SB, Phuleria H, Fine PM, Sioutas C. 2005. Measurements of particle number and mass concentrations and size distributions in a tunnel environment. Environ Sci Technol 39(22):8653–8663, PMID: 16323759, https://doi.org/10.1021/es050360s.

Gerlofs-Nijland ME, Totlandsdal AI, Kilinç E, Boere AJ, Fokkens PH, Leseman DL, et al. 2010. Pulmonary and cardiovascular effects of traffic-related particulate matter: 4-week exposure of rats to roadside and diesel engine exhaust particles. Inhal Toxicol 22(14):1162–1173, PMID: 21126152, https://doi.org/10.3109/08958378.2010.531062.

Ghorani-Azam A, Riahi-Zanjani B, Balali-Mood M. 2016. Effects of air pollution on human health and practical measures for prevention in Iran. J Res Med Sci 21(1):65, https://doi.org/10.4103/1735-1995.189646.

Ginzburg H, Liu X, Baker M, Shreeve R, Jayanty RK, Campbell D, et al. 2015. Monitoring study of the near-road pm2.5 concentrations in Maryland. J Air Waste Manag Assoc 65(9):1062–1071, PMID: 26067547, https://doi.org/10.1080/10962247.2015.1056887.

Gochfeld M. 2017. Sex differences in human and animal toxicology. Toxicol Pathol 45(1):172–189, PMID: 27895264, https://doi.org/10.1177/0192623316677327.

Goldfarbmuren KC, Jackson ND, Sajuthi SP, Dyjack N, Li KS, Rios CL, et al. 2020. Dissecting the cellular specificity of smoking effects and reconstructing lineages in the human airway epithelium. Nat Commun 11(1):2485, PMID: 32427931, https://doi.org/10.1038/s41467-020-16239-z.

Grigoratos T, Martini G. 2015. Brake wear particle emissions: a review. Environ Sci Pollut Res Int 22(4):2491–2504, PMID: 25318420, https://doi.org/10.1007/s11356-014-3696-8.

Gross DS, Galli ME, Silva PJ, Wood SH, Liu D-Y, Prather KA. 2000. Single particle characterization of automobile and diesel truck emissions in the Caldecott tunnel. Aerosol Sci Technol 32(2):152–163, https://doi.org/10.1080/027868200303858.
Han ES, Muller FL, Pérez VI, Qi W, Liang H, Xi L, et al. 2008. The in vivo gene expression signature of oxidative stress. Physiol Genomics 34(1):112–126, PMID: 18445702, https://doi.org/10.1152/physiolgenomics.00239.2007.
Han X, Naeher LP. 2006. A review of traffic-related air pollution exposure assessment studies in the developing world. Environ Int 32(1):106–120, PMID: 16005066, https://doi.org/10.1016/j.envint.2005.05.020.
Hinderer S, Schenke-Layland K. 2019. Cardiac fibrosis–a short review of causes and therapeutic strategies. Adv Drug Deliv Rev 146:77–82, PMID: 31158407, https://doi.org/10.1016/j.addr.2019.05.011.
Hong YC, Lee JT, Kim H, Kwon HJ. 2002. Air pollution: a new risk factor in ischemic stroke mortality. Stroke 33(9):2165–2169, PMID: 12215581, https://doi.org/10.1161/01.str.0000026865.52610.5b.
Johannson KA, Balmes JR, Collard HR. 2015. Air pollution exposure: a novel environmental risk factor for interstitial lung disease? Chest 147(4):1161–1167, PMID: 25846532, https://doi.org/10.1378/chest.14-1299.
Kagan VE, Kapralov AA, St Croix CM, Watkins SC, Kisin ER, Kotchey GP, et al. 2014. Lung macrophages "digest" carbon nanotubes using a superoxide/peroxynitrite oxidative pathway. ACS Nano 8(6):5610–5621, PMID: 24871084, https://doi.org/10.1021/nn406484b.
Kamo N, Ke B, Ghaffari AA, Shen XD, Busuttil RW, Cheng G, et al. 2013. ASC/caspase-1/IL-1β signaling triggers inflammatory responses by promoting HMGB1 induction in liver ischemia/reperfusion injury. Hepatology 58(1):351–362, PMID: 23408710, https://doi.org/10.1002/hep.26320.
Kayalar O, Oztay F, Ongen HG. 2020. Gastrin-releasing peptide induces fibrotic response in MRC5s and proliferation in A549s. Cell Commun Signal 18(1):96, PMID: 32552754, https://doi.org/10.1186/s12964-020-00585-y.
Kelly FJ. 2003. Oxidative stress: its role in air pollution and adverse health effects. Occup Environ Med 60(8):612–616, PMID: 12883027, https://doi.org/10.1136/oem.60.8.612.
Kim H, Noh J, Noh Y, Oh SS, Koh SB, Kim C. 2019. Gender difference in the effects of outdoor air pollution on cognitive function among elderly in Korea. Front Public Health 7:375, PMID: 31921740, https://doi.org/10.3389/fpubh.2019.00375.
Krzyzanowski M, Cohen A. 2008. Update of WHO air quality guidelines. Air Qual Atmos Health 1:7–13, https://doi.org/10.1007/s11869-008-0008-9.
Kuykendall JR, Shaw SL, Paustenbach D, Fehling K, Kacew S, Kabay V. 2009. Chemicals present in automobile traffic tunnels and the possible community health hazards: a review of the literature. Inhal Toxicol 21(9):747–792, PMID: 19555229, https://doi.org/10.1080/08958370802524357.
Larsson BM, Grunewald J, Sköld CM, Lundin A, Sandström T, Eklund A, et al. 2010. Limited airway effects in mild asthmatics after exposure to air pollution in a road tunnel. Respir Med 104(12):1912–1918, PMID: 20621461, https://doi.org/10.1016/j.rmed.2010.06.014.
Larsson BM, Sehlstedt M, Grunewald J, Sköld CM, Lundin A, Blomberg A, et al. 2007. Road tunnel air pollution induces bronchoalveolar inflammation in healthy subjects. Eur Respir J 29(4):699–705, PMID: 17251238, https://doi.org/10.1183/09031936.00035706.
Lee B-K, Kim Y. 2014. Sex-specific profiles of blood metal levels associated with metal–iron interactions. Saf Health Work 5(3):113–117, PMID: 25379323, https://doi.org/10.1016/j.shaw.2014.06.005.
Lippmann M, Ito K, Hwang JS, Maciejczyk P, Chen LC. 2006. Cardiovascular effects of nickel in ambient air. Environ Health Perspect 114:1662–1669, PMID: 17107850, https://doi.org/10.1289/ehp.9150.
Lodovici M, Bigagli E. 2011. Oxidative stress and air pollution exposure. J Toxicol 2011:1–9, https://doi.org/10.1155/2011/487074.
Lough GC, Schauer JJ, Park J-S, Shafer MM, DeMinter JT, Weinstein JP. 2005. Emissions of metals associated with motor vehicle roadways. Environ Sci Technol 39(3):826–836, PMID: 15757346, https://doi.org/10.1021/es048715f.
Manning MI, Martin RV, Hasenkopf C, Flasher J, Li C. 2018. Diurnal patterns in global fine particulate matter concentration. Environ Sci Technol Lett 5(11):687–691, https://doi.org/10.1021/acs.estlett.8b00573.
Mao K, Quipildor GF, Tabrizian T, Novaj A, Guan F, Walters RO, et al. 2018. Late-life targeting of the IGF-1 receptor improves healthspan and lifespan in female mice. Nat Commun 9(1):2394, PMID: 29921922, https://doi.org/10.1038/s41467-018-04805-5.
McClure CD, Jaffe DA. 2018. Us particulate matter air quality improves except in wildfire-prone areas. Proc Natl Acad Sci USA 115(31):7901–7906, PMID: 30012611, https://doi.org/10.1073/pnas.1804353115.
Münzel T, Sørensen M, Gori T, Schmidt FP, Rao X, Brook FR, et al. 2017a. Environmental stressors and cardio-metabolic disease: part II-mechanistic insights. Eur Heart J 38(8):557–564, PMID: 27460891, https://doi.org/10.1093/eurheartj/ehw294.
Münzel T, Sørensen M, Gori T, Schmidt FP, Rao X, Brook J, et al. 2017b. Environmental stressors and cardio-metabolic disease: part I-epidemiologic evidence supporting a role for noise and air pollution and effects of mitigation strategies. Eur Heart J 38(8):550–556, PMID: 27460892, https://doi.org/10.1093/eurheartj/ehw269.
Nakahara H, Song J, Sugimoto M, Hagihara K, Kishimoto T, Yoshizaki K, et al. 2003. Anti-interleukin-6 receptor antibody therapy reduces vascular endothelial growth factor production in rheumatoid arthritis. Arthritis Rheum 48(6):1521–1529, PMID: 12794819, https://doi.org/10.1002/art.11143.
Newby DE, Mannucci PM, Tell GS, Baccarelli AA, Brook RD, Donaldson K, et al. 2015. Expert position paper on air pollution and cardiovascular disease. Eur Heart J 36(2):83–93b, PMID: 25492627, https://doi.org/10.1093/eurheartj/ehu458.
Nguyen T, Nioi P, Pickett CB. 2009. The Nrf2-antioxidant response element signaling pathway and its activation by oxidative stress. J Biol Chem 284(20):13291–13295, PMID: 19182219, https://doi.org/10.1074/jbc.R900010200.
Ning Q, Li F, Wang L, Li H, Yao Y, Hu T, et al. 2018. S100A4 amplifies TGF-β-induced epithelial-mesenchymal transition in a pleural mesothelial cell line. J Investig Med 66(2):334–339, PMID: 29141874, https://doi.org/10.1136/jim-2017-000542.
Oh M-H, Oh SY, Yu J, Myers AC, Leonard WJ, Liu YJ, et al. 2011. IL-13 induces skin fibrosis in atopic dermatitis by thymic stromal lymphopoietin. J Immunol 186(12):7232–7242, PMID: 21576506, https://doi.org/10.4049/jimmunol.1100504.
O'Leary NA, Wright MW, Brister JR, Ciufo S, Haddad D, McVeigh R, et al. 2016. Reference sequence (RefSeq) database at NCBI: current status, taxonomic expansion, and functional annotation. Nucleic Acids Res 44(D1):D733–D745, PMID: 26553804, https://doi.org/10.1093/nar/gkv1189.
Padró-Martínez LT, Patton AP, Trull JB, Zamore W, Brugge D, Durant JL. 2012. Mobile monitoring of particle number concentration and other traffic-related air pollutants in a near-highway neighborhood over the course of a year. Atmos Environ (1994) 61:253–264, PMID: 23144586, https://doi.org/10.1016/j.atmosenv.2012.06.088.
Pandya K, Kim HS, Smithies O. 2006. Fibrosis, not cell size, delineates beta-myosin heavy chain reexpression during cardiac hypertrophy and normal aging in vivo. Proc Natl Acad Sci USA 103(45):16864–16869, PMID: 17068123, https://doi.org/10.1073/pnas.0607700103.
Patten KT, González EA, Valenzuela A, Berg E, Wallis C, Garbow JR, et al. 2020. Effects of early life exposure to traffic-related air pollution on brain development in juvenile Sprague-Dawley rats. Transl Psychiatry 10(1):166, PMID: 32483143, https://doi.org/10.1038/s41398-020-0845-3.
Piguet PF, Grau GE, Vassalli P. 1990. Subcutaneous perfusion of tumor necrosis factor induces local proliferation of fibroblasts, capillaries, and epidermal cells, or massive tissue necrosis. Am J Pathol 136(1):103–110, PMID: 1688687.
Pilling D, Vakil V, Cox N, Gomer RH. 2015. TNF-α-stimulated fibroblasts secrete lumican to promote fibrocyte differentiation. Proc Natl Acad Sci USA 112(38):11929–11934, PMID: 26351669, https://doi.org/10.1073/pnas.1507387112.
Rao X, Asico LD, Zanos P, Mahabeleshwar GH, Singh Gangwar R, Xia C, et al. 2019. Alpha2B-adrenergic receptor overexpression in the brain potentiate air pollution-induced behavior and blood pressure changes. Toxicol Sci 169(1):95–107, PMID: 30812033, https://doi.org/10.1093/toxsci/kfz025.
Rao X, Zhong J, Maiseyeu A, Gopalakrishnan B, Villamena FA, Chen L-C, et al. 2014. CD36-dependent 7-ketocholesterol accumulation in macrophages mediates progression of atherosclerosis in response to chronic air pollution exposure. Circ Res 115(9):770–780, PMID: 25186795, https://doi.org/10.1161/CIRCRESAHA.115.304666.
Ruggieri A, Anticoli S, D'Ambrosio A, Giordani L, Viora M. 2016. The influence of sex and gender on immunity, infection and vaccination. Ann Ist Super Sanita 52(2):198–204, PMID: 27364394, https://doi.org/10.4415/ANN_16_02_11.
Sawyer DB. 2011. Oxidative stress in heart failure: what are we missing? Am J Med Sci 342(2):120–124, PMID: 21747279, https://doi.org/10.1097/MAJ.0b013e3182249fcd.
Schnelle-Kreis J, Küpper U, Sklorz M, Cyrys J, Briedé JJ, Peters A, et al. 2009. Daily measurement of organic compounds in ambient particulate matter in Augsburg, Germany: new aspects on aerosol sources and aerosol related health effects. Biomarkers 14(suppl 1):39–44, https://doi.org/10.1080/13547500902965997.
Shaddick G, Thomas ML, Mudu P, Ruggeri G, Gumy S. 2020. Half the world's population are exposed to increasing air pollution. npj Clim Atmos Sci 3(1):23, https://doi.org/10.1038/s41612-020-0124-2.
Shang Y, Sun Q. 2018. Particulate air pollution: major research methods and applications in animal models. Environ Dis 3(3):57–62, PMID: 31549002, https://doi.org/10.4103/ed.ed_16_18.
Solomon PA, Crumpler D, Flanagan JB, Jayanty RK, Rickman EE, McDade CE. 2014. U.S. national $PM_{2.5}$ Chemical Speciation Monitoring Networks-CSN and IMPROVE: description of networks. J Air Waste Manag Assoc 64(12):1410–1438, PMID: 25562937, https://doi.org/10.1080/10962247.2014.956904.
Stockfelt L, Andersson EM, Molnár P, Gidhagen L, Segersson D, Rosengren A, et al. 2017. Long-term effects of total and source-specific particulate air pollution on incident cardiovascular disease in Gothenburg, Sweden. Environ Res 158:61–71, PMID: 28600978, https://doi.org/10.1016/j.envres.2017.05.036.
Suh HH, Bahadori T, Vallarino J, Spengler JD. 2000. Criteria air pollutants and toxic air pollutants. Environ Health Perspect 108:625–633, PMID: 10940240, https://doi.org/10.2307/3454398.
Sun Q, Yue P, Ying Z, Cardounel AJ, Brook RD, Devlin R, et al. 2008. Air pollution exposure potentiates hypertension through reactive oxygen species-mediated

activation of Rho/ROCK. Arterioscler Thromb Vasc Biol 28(10):1760–1766, PMID: 18599801, https://doi.org/10.1161/ATVBAHA.108.166967.
Svartengren M, Strand V, Bylin G, Järup L, Pershagen G. 2000. Short-term exposure to air pollution in a road tunnel enhances the asthmatic response to allergen. Eur Respir J 15(4):716–724, PMID: 10780764, https://doi.org/10.1034/j.1399-3003.2000.15d15.x.
Svingen T, Letting H, Hadrup N, Hass U, Vinggaard AM. 2015. Selection of reference genes for quantitative RT-PCR (RT-qPCT) analysis of rat tissues under physiological and toxicological conditions. PeerJ 3:e855, PMID: 25825680, https://doi.org/10.7717/peerj.855.
Takano APC, Justo LT, Dos Santos NV, Marquezini MV, de André PA, da Rocha FMM, et al. 2019. Pleural anthracosis as an indicator of lifetime exposure to urban air pollution: an autopsy-based study in Sao Paulo. Environ Res 173:23–32, PMID: 30884435, https://doi.org/10.1016/j.envres.2019.03.006.
Travers JG, Kamal FA, Robbins J, Yutzey KE, Blaxall BC. 2016. Cardiac fibrosis: the fibroblast awakens. Circ Res 118(6):1021–1040, PMID: 26987915, https://doi.org/10.1161/CIRCRESAHA.115.306565.
U.S. EPA (U.S. Environmental Protection Agency). 2013. January national ambient air quality standards for particulate matter. Docket No. EPA-HQ-OAR-2007-0492, FRL-9761-8, RIN2060-AO47. Fed Reg 78:3085–3287, https://www.federalregister.gov/documents/2013/01/15/2012-30946/national-ambient-air-quality-standards-for-particulate-matter [accessed 30 November 2020].
Vahter M, Gochfeld M, Casati B, Thiruchelvam M, Falk-Filippson A, Kavlock R, et al. 2007. Implications of gender differences for human health risk assessment and toxicology. Environ Res 104(1):70–84, PMID: 17098226, https://doi.org/10.1016/j.envres.2006.10.001.
Vatner SF, Pachon RE, Vatner DE. 2015. Inhibition of adenylyl cyclase type 5 increases longevity and healthful aging through oxidative stress protection. Oxid Med Cell Longev 2015:250310, PMID: 25945149, https://doi.org/10.1155/2015/250310.
Vouk VB, Piver WT. 1983. Metallic elements in fossil fuel combustion products: amounts and form of emissions and evaluation of carcinogenicity and mutagenicity. Environ Health Perspect 47:201–225, PMID: 6337825, https://doi.org/10.1289/ehp.8347201.
Wang G, Hamid T, Keith RJ, Zhou G, Partridge CR, Xiang X, et al. 2010. Cardioprotective and antiapoptotic effects of heme oxygenase-1 in the failing heart. Circulation 121(17):1912–1925, https://doi.org/10.1161/CIRCULATIONAHA.109.905471.
Wilbur S, Abadin H, Fay M, Yu D, Tencza B, Ingerman L, et al. 2012. Toxicological Profile for Chromium. Atlanta, GA: Agency for Toxic Substances and Disease Registry.
Wold LE, Ying Z, Hutchinson KR, Velten M, Gorr MW, Velten C, et al. 2012. Cardiovascular remodeling in response to long-term exposure to fine particulate matter air pollution. Circ Heart Fail 5(4):452–461, PMID: 22661498, https://doi.org/10.1161/CIRCHEARTFAILURE.112.966580.
World Health Organization Occupational and Environmental Health Team. 2006. WHO Air Quality Guidelines for Particulate Matter, Ozone, Nitrogen Dioxide and Sulfur Dioxide: Global Update 2005: Summary of Risk Assessment, https://apps.who.int/iris/handle/10665/69477 [accessed 30 November 2020].
Xu H, Chen J, Zhao Q, Zhang Y, Wang T, Feng B, et al. 2019. Ambient air pollution is associated with cardiac repolarization abnormalities in healthy adults. Environ Res 171:239–246, PMID: 30690270, https://doi.org/10.1016/j.envres.2019.01.023.
Xu X, Yavar Z, Verdin M, Ying Z, Mihai G, Kampfrath T, et al. 2010. Effect of early particulate air pollution exposure on obesity in mice: role of p47phox. Arterioscler Thromb Vasc Biol 30(12):2518–2527, PMID: 20864666, https://doi.org/10.1161/ATVBAHA.110.215350.
Yan L, Vatner DE, O'Connor JP, Ivessa A, Ge H, Chen W, et al. 2007. Type 5 adenylyl cyclase disruption increases longevity and protects against stress. Cell 130(2):247–258, PMID: 17662940, https://doi.org/10.1016/j.cell.2007.05.038.
Ying Z, Yue P, Xu X, Zhong M, Sun Q, Mikolaj M, et al. 2009. Air pollution and cardiac remodeling: a role for RhoA/Rho-kinase. Am J Physiol Heart Circ Physiol 296(5):H1540–H1550, PMID: 19286943, https://doi.org/10.1152/ajpheart.01270.2008.
Zhang K, Batterman S. 2013. Air pollution and health risks due to vehicle traffic. Sci Total Environ 450–451:307–316, PMID: 23500830, https://doi.org/10.1016/j.scitotenv.2013.01.074.
Zhou S, Yuan Q, Li W, Lu Y, Zhang Y, Wang W. 2014. Trace metals in atmospheric fine particles in one industrial urban city: spatial variations, sources, and health implications. J Environ Sci (China) 26(1):205–213, PMID: 24649708, https://doi.org/10.1016/S1001-0742(13)60399-X.